Quantification of karst aquifer discharge components during storm events through end-member mixing analysis using natural chemistry and stable isotopes as tracers

Daniel H. Doctor · E. Calvin Alexander Jr · Metka Petrič · Janja Kogovšek · Janko Urbanc · Sonja Lojen · Willibald Stichler

Abstract Karst aquifer components that contribute to the discharge of a water supply well in the Classical Karst (Kras) region (Italy/Slovenia) were quantitatively estimated during storm events. Results show that water released from storage within the epikarst may comprise as much as two-thirds of conduit flow in a karst aquifer following rainfall. Principal components analysis (PCA) and end-member mixing analysis (EMMA) were performed using major ion chemistry and the stable isotopes of water ($\delta^{18}O$, $\delta^{2}H$) and of dissolved inorganic carbon ($\delta^{13}C_{DIC}$) to estimate mixing proportions among three sources: (1) allogenic river recharge, (2) autogenic recharge, and (3) an anthropogenic component stored within the epikarst. The sinking river most influences the chemical composition of the water-supply well under low-flow conditions; however, this proportion changes rapidly during recharge events. Autogenic recharge water, released from shallow storage in the epikarst, displaces the river water and is observed at the well within hours after the onset of precipitation. The autogenic recharge end member is the second largest component of the well chemistry, and its contribution increases with higher flow. An anthropogenic component derived from epikarstic storage also impacts the well under conditions of elevated hydraulic head, accounting for the majority of the chemical response at the well during the wettest conditions.

Résumé La composante des aquifères karstiques contribuant au débit des puits d'alimentation en eau potable dans la région de Kras (Italie/Slovénie) a été estimée quantitativement durant les évènements de crues. Les résultats montrent que l'eau relarguée par l'épikarst peut contenir jusqu'aux deux-tiers du débit du conduit karstique, après un évènement pluvieux. Une analyse en composante principale (PCA) et une analyse EMMA (End-Member Mixing Analysis) ont été réalisées en utilisant les ions majeurs et les isotopes stables de l'eau ($\delta^{18}O$, $\delta^{2}H$) et de la matière organique ($\delta^{13}C_{DIC}$) pour estimer les proportions de mélange entre les trois sources (1) la recharge allogénique par la rivière (2) la recharge autogénique (3) la composant anthropique de l'épikarst. La rivière influence essentiellement la composition de chimique des puits lors des basses eaux; par contre la proportion change rapidement lors des évènements de recharge. La recharge autogénique, en provenance des eaux de l'épikarst superficiel, déplace les eaux de la rivière et est observée dans les heures qui suit le début de la précipitation. La recharge autogénique est la deuxième plus importante composante chimique de l'eau du puits, et son influence grandit avec le débit. La composante anthropogénique est dérivée du réservoir épikarstique influençant le puits lorsque la charge hydraulique est la plus haute, et justifiant la majorité des réponses chimiques du puits durant les conditions les plus humides.

Resumen Se estimaron cuantitativamente, durante eventos lluviosos, los componentes de un acuífero kárstico que contribuyen a la descarga de un pozo de abastecimiento de agua en la región Kras (Italia/Eslovenia). Los resultados muestran que el agua liberada del reservorio dentro de la zona epikárstica puede comprender hasta dos tercios del

Received: 28 October 2004 / Accepted: 20 February 2006
Published online: 11 July 2006

D. H. Doctor · E. C. Alexander Jr
Department of Geology and Geophysics,
University of Minnesota,
310 Pillsbury Dr. SE, Minneapolis, MN 55455, USA

M. Petrič · J. Kogovšek
Karst Research Institute,
Titov trg 2, Postojna, Slovenia

J. Urbanc
Geological Survey of Slovenia,
Dimičeva 14, Ljubljana, Slovenia

S. Lojen
Jožef Stefan Research Institute,
39 Jamova Cesta, Ljubljana, Slovenia

W. Stichler
GSF Institute of Hydrology,
Ingolstädter Landstr. 1, Neuherberg, Germany

D. H. Doctor (✉)
US Geological Survey,
345 Middlefield Rd., Menlo Park, CA 94025, USA
e-mail: dhdoctor@usgs.gov
Tel.: +1-650-3294544
Fax: +1-650-3294568

 DOI 10.1007/s10040-006-0031-6

flujo en conductos en un acuífero kárstico después de la lluvia. Se realizaron un Análisis de Componentes Principales (PCA) y un Análisis de Mezcla de Miembros Extremos (EMMA) usando química de iones y los isótopos estables del agua ($\delta^{18}O$, $\delta^{2}H$) y carbono inorgánico disuelto ($\delta^{13}C_{DIC}$) para estimar las proporciones de mezcla entre las tres fuentes: (1) recarga de río alogénico, (2) recarga autogénica, y (3) un componente antropogénico almacenado en el epikarst. La composición química del agua del pozo de abastecimiento está influenciada principalmente por el río hundido bajo condiciones de flujo escaso; sin embargo, esta proporción cambia mucho durante eventos de recarga. La recarga de agua autogénica, liberada del almacenamiento somero en el epikarst, desplaza el agua de río y se detecta en el pozo a pocas horas después del inicio de la lluvia. La recarga autogénica del miembro extremo es el segundo componente más grande de la química del agua y su contribución se incremente con flujos altos. Un componente antropogénico derivado del almacenamiento epikárstico también impacta el pozo bajo condiciones de elevada presión hidráulica explicando la mayor parte de la respuesta química en el pozo durante las condiciones más húmedas.

Keywords Karst · Hydrochemistry · Stable isotopes · Statistical modeling · Groundwater/surface-water relations

Introduction

Quantitative understanding of the hydrologic functioning in karst aquifers is necessary to manage water resources and develop aquifer protection and remediation strategies. In order to identify the sources and flowpaths of water contributing to karst aquifer discharge, artificial tracers such as fluorescent dyes are often introduced into points of focused recharge and are measured at the presumed points of outlet (Ford and Williams 1989). Water tracing in this way is critical for delineating flowpaths within karst aquifers, but is less effective for the study of interactions between the diffuse and fast-flow portions of karst aquifers, or between phreatic and unsaturated (epikarst) zones. Fortunately, natural environmental stables isotopes in conjunction with other geochemical parameters are useful tools in cases where artificial tracing is not feasible such as at the scale of a regional aquifer system.

Several prior studies have applied environmental isotopes of water ($\delta^{18}O$, $\delta^{2}H$, ^{3}H) to estimate mixing between source components in karst aquifers (e.g., Lakey and Krothe 1996; Maloszewski et al. 2002; Perrin et al. 2003). Water isotopes are excellent conservative tracers; however, interpretation of mixing models involving a limited number of tracers is often ambiguous. In this study, multiple water chemistry and environmental stable isotope parameters ($\delta^{18}O$, $\delta^{2}H$, $\delta^{13}C_{DIC}$) have been used as tools to estimate proportions of various groundwater sources that supply the discharge of a water-supply well under changing hydrologic conditions within a regionally important karst aquifer in southwestern Slovenia.

Principal components analysis (PCA) and end-member mixing analysis (EMMA) were performed on chemical and isotopic data collected frequently (daily or more than once per day) during storm events in two separate years. PCA is a multivariate statistical technique for the reduction of correlations among many variables into a smaller number of factors that account for the majority of the variance in the original data. EMMA is a technique that estimates the proportions of known or hypothetical source solutions that combine to produce the chemistry measured at the point of discharge. Through the PCA/EMMA approach, a multitude of natural tracers may be considered in unison within a mixing model, thus retaining information from all measured parameters. Here, fractions of the end-member source solutions were estimated for each water sample collected during individual storm events, permitting a high-resolution time series record of changing source contributions under variable hydrologic conditions. This information is beneficial for well-head protection strategies, and to prevent water deliveries that may be potentially deleterious to public health. In addition, the results elucidate some general facets of karst aquifer functioning with respect to water release from the epikarst following recharge events.

Background

The study site is located within the Classical Karst region (or Kras) of southwestern Slovenia and north of Trieste, Italy, and is shown in Fig. 1. The Kras region is a high limestone plateau that rises above the Adriatic Sea at the Gulf of Trieste, consisting of a stratigraphic sequence of limestones and dolomites overlain by argillaceous turbidite sediments (flysch) that has been tectonically uplifted and overturned (Cucchi et al. 1987). The autogenic recharge area of the Kras is approximately 40 km long, up to 13 km wide, and covers roughly 440 km^2 (Kranjc 1997). Mean annual precipitation is between 1,400 and 1,600 mm (Kranjc 1997). Rainfall readily infiltrates into the karstified bedrock, due to thin soils (0–0.5 m) and the abundance of exposed limestone bedrock surfaces. Sparse freshwater resources exist on the surface of the Slovene Kras. There are no lakes, no surface streams, and only a few small retention ponds. There is, however, a large regional aquifer stored within the limestone bedrock, yielding an estimated 1,100 million m^3 of groundwater discharge annually (Civita et al. 1995). On the northwestern side of the Kras the groundwater of the regional aquifer resurges in a narrow zone as a result of the west-southwest dip of the rock layers (Fig. 1). Past hydrogeological research on the Kras has focused mainly on the Timavo springs, the largest natural source of groundwater in the region (Galli 1999). Collectively, the average discharge of the Timavo springs is approximately 30.2 m^3/s (variable within the years studied between 18 and 39.4 m^3/s), with low flows averaging around 9 m^3/s, and maximum flows over 130 m^3/s (Gemiti 1984a). The Timavo springs were the primary source of water supply

 DOI 10.1007/s10040-006-0031-6

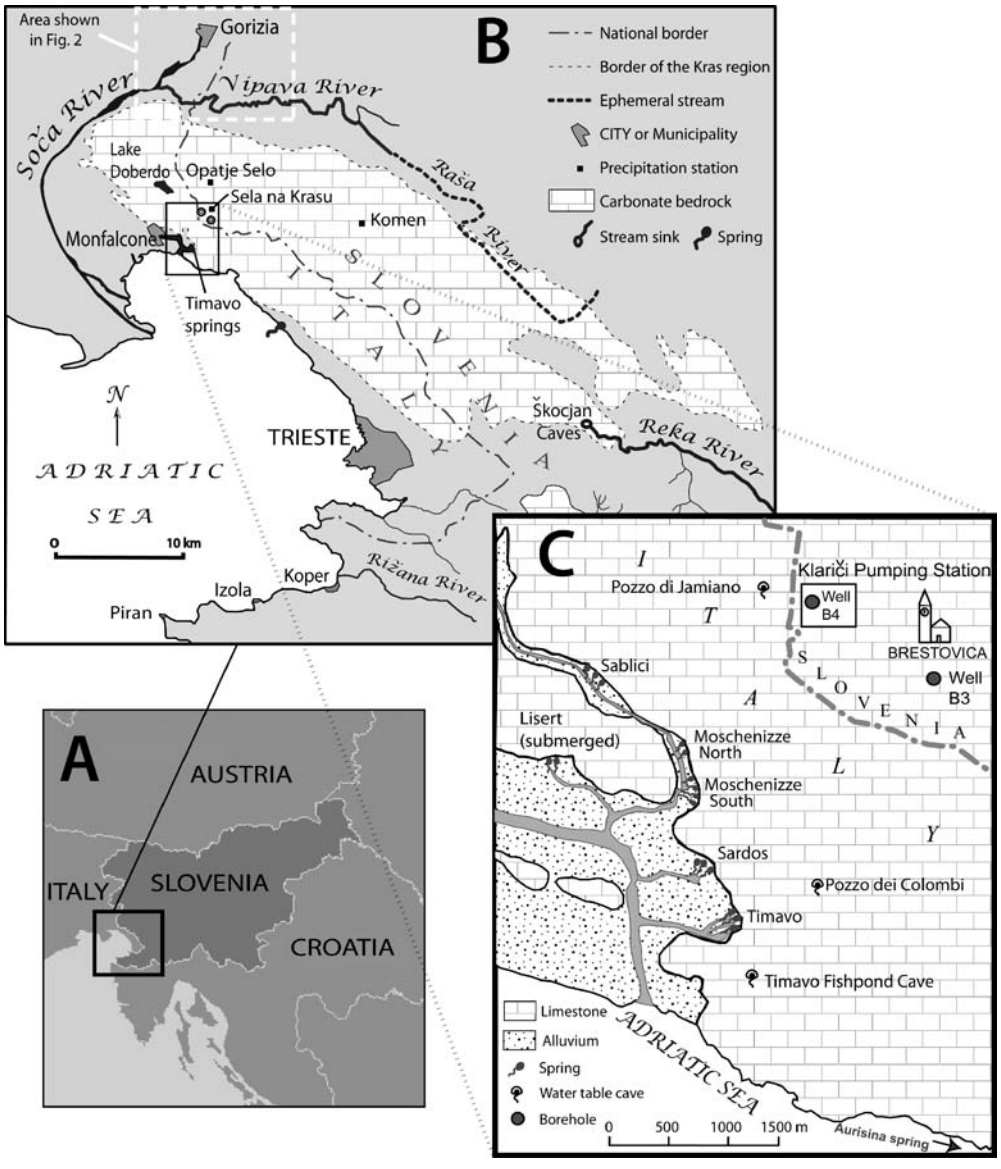

Fig. 1 Map showing the major hydrogeological features of the Kras region (modified from Krivic 1981). The *enlarged region* in panel C shows the location of the Klariči pumping station and monitoring wells B-4 and well B-3. The *dashed box* at the top of panel B indicates the outline of the region shown in Fig. 2

for the city of Trieste, Italy until a series of wells was completed in the alluvial aquifer of the Soča River in Italy (ACEGA Trieste 1988). The Timavo springs, as well as other smaller springs located nearby, are shown in Fig. 1.

Two major allogenic sources of water contribute to the Kras aquifer. On the southeast border, the Reka River flows on flysch terrain from its eastern source in Croatia until it encounters the limestone bedrock of the Kras. At this contact, it sinks at the dramatic Škocjan Caves (a UNESCO World Heritage site), mixes with the autogenic recharge of the Kras aquifer, and emerges again at the Timavo springs (Timeus 1928; Gemiti 1984b). On the northwestern edge of the Kras, the alluvial deposits of the Soča River cover the carbonate bedrock and form a separate aquifer system. Several authors have posited connection between the Soča River alluvial aquifer and the karst aquifer of the Kras (Mosetti and D'Ambrosi 1963; Flora and Longinelli 1989, Urbanc and Kristan 1998). Losses of the Soča River's discharge have been gaged downstream of the city of Gorizia (Fig. 2). Estimates of flow loss are on the order of 20–25 m^3/s, approximately 10% of the river's total discharge upstream at Gorizia during average flow conditions (Mosetti and D'Ambrosi 1963; ACEGA Trieste 1988). Concurrent measurements of the water chemistry and oxygen stable isotopic composition ($\delta^{18}O$) of the Soča River and the nearby karst groundwaters suggest that the Soča River has a widespread influence on the Kras aquifer (Gemiti and Licciardello 1977; Longinelli 1988; Flora and Longinelli 1989; Urbanc and Kristan 1998; Krokos 1998; Doctor 2002).

The Klariči water supply

The water supply for the 25,000 inhabitants of the upper Slovenian Kras plateau comes from the Klariči pumping station located towards the northwestern edge of the Kras near the resurgence zone of the regional aquifer. Annual

 DOI 10.1007/s10040-006-0031-6

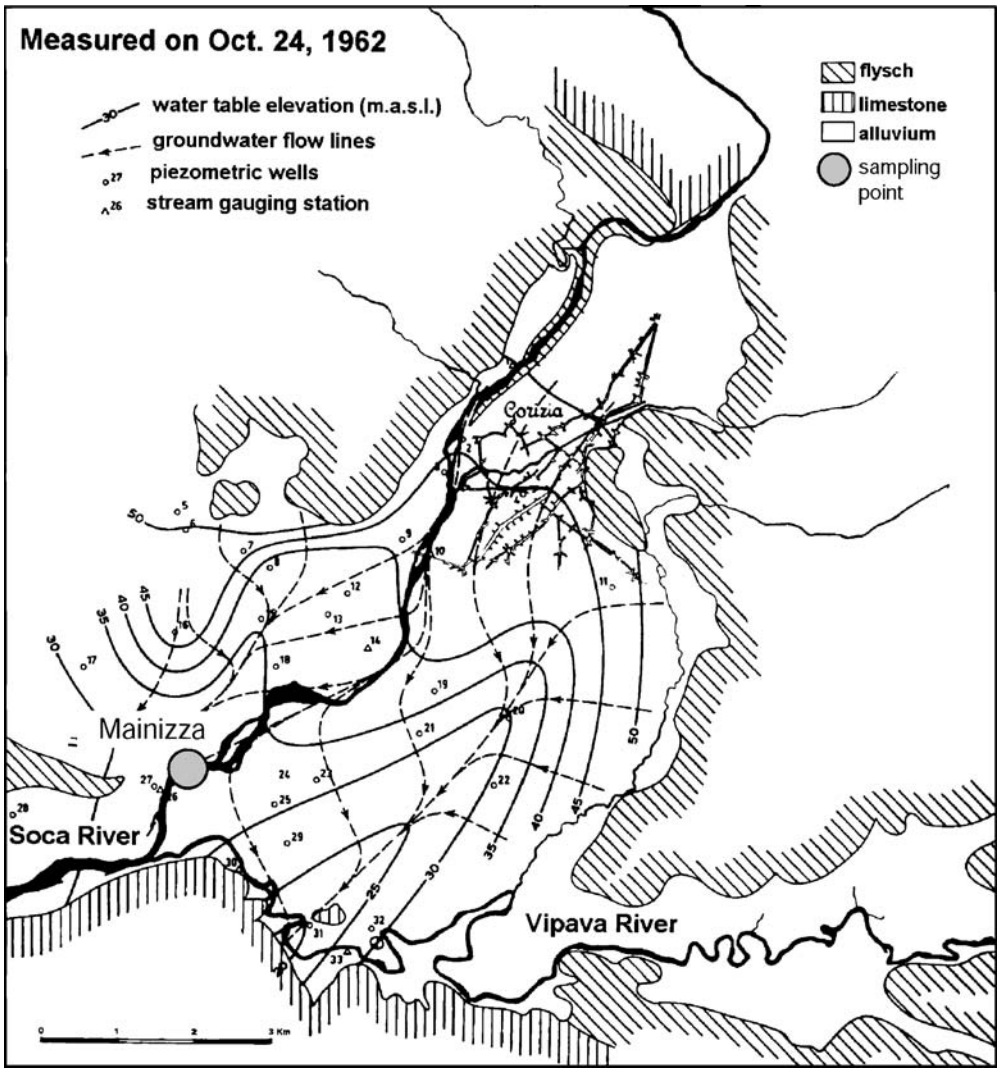

Fig. 2 Piezometric map of the Soča River plain, indicating zones of focused ground water loss flanking the river (from Mosetti and D'Ambrosi 1963). The sampling point at Mainizza is shown for reference

consumption of water from this source is currently around 1,700,000 m^3, and 30–130 l/s is routinely distributed to the supply system (Petrič and Kogovšek 2000). The Klariči pumping station consists of three pumping wells and one monitoring well within a radius of less than 10 m. The monitoring well was the primary sampling point for this study. Hereafter this sampling point shall be referred to as borehole or well B-4, in keeping with the notation of Krivic (1982). More than 1 m of the borehole B-4 intersects an open conduit, and the production wells draw water from the same conduit. Depth to the water table fluctuates due to changes in pumping rate; however, on average the water table is approximately 2.0 m above sea level (m a.s.l.). Details of the monitoring well construction are given in Table 1.

A pumping test conducted with simultaneous sampling of chemical and isotopic parameters in mid-August of 1995 yielded up to 250 L/s and caused drawdown of only 0.5 m (Urbanc and Kristan 1998). Chemical monitoring during the 1995 pumping test demonstrated that no seawater intrusion occurred, and it was estimated that approximately 50% of the water produced during the

Table 1 Well log and pump test data for well B-4 and well B-3

	Monitoring well B-4	Monitoring well B-3
Surface elevation (above sea level)	18.0 m a.s.l.	40.0 m a.s.l
Total depth (below sea level)	52.5 m b.s.l. (open fracture from 41.7–43.0 m b.s.l.)	44.6 m b.s.l.
Screen interval	14–68 m depth	Unknown
Water table elevation (range)	0.5–3.5 m a.s.l.	<0.0–3.0 m a.s.l.
Transmissivity (T)	$>1\times10^{-1}$ m^2/s	2×10^{6} m^2/s
Hydraulic conductivity (K)	$>8\times10^{-4}$ m/s	4×10^{-7} m/s
Geologic material	0–0.5 m soil	0–2 m soil
	0.5–52.5 m Cretaceous limestone	2–85.3 m Cretaceous limestone

 DOI 10.1007/s10040-006-0031-6

pumping test at well B-4 was derived from the Soča River, located a few kilometers west of the pumping station, based on concurrent oxygen stable isotopic measurements of the river and well water (Urbanc and Kristan 1998).

A second borehole, well B-3, is located approximately 1.5 km to the southeast of the Klariči pumping station and was repeatedly sampled during this study. This well is a partially cased borehole of 85.3 m; depth to water during sampling ranged from 38 to 50 m. In August of 1999, the well was dry and the bottom was reached at a depth of 50 m below the surface, indicating that the well intersects a zone of local water level fluctuation. Normally, the water level in the well at the time of sampling was between 2.0 and 3.0 m a.s.l. A pump test at well B-3 revealed transmissivity (2×10^{-6} m^2/s) and a hydraulic conductivity (4×10^{-7} m/s) several orders of magnitude lower than at well B-4 (Krivic 1981). Recognizing that pump test results often do not accurately represent the properties of a karst aquifer (White 1988), these results are presented to emphasize the high degree of heterogeneity observed over a relatively short distance (1 km) in this system. Nevertheless, from April 1977 to January 1980, continuous phreatic water level measurements were made in well B-4 and well B-3, and the coefficient of cross-correlation between the two time series was 0.99 (Krivic 1982). Previous work has demonstrated that the strong degree of karst development throughout the bedrock permits continuous hydraulic connection within the aquifer in spite of local differences in transmissivity.

A few natural shafts nearby to the Klariči pumping station intersect the shallow groundwater stored within the epikarst. Two of these are the 'Cave East of the Train Station' and the 'Timavo Fishpond Cave', both located in Italy. The Cave East of the Train Station is near the train station in the town of Monfalcone. This shaft has been observed to contain water at an elevation of 15.5 m a.s.l. and which exhibits a chemistry that is elevated in Cl^- (up to 36 mg/L) and SO_4^{2-} (up to 22 mg/L) with respect to the other local groundwaters (Cancian 1987). Despite the proximity to the sea, the chemistry of water in this shaft is not consistent with a seawater source (Cancian 1987). Moreover, during a flood in April 1987, this shaft showed the presence of Strep Group D (SGD) enterococcal bacteria, and two types of *Pseudomonas fluorescens*, with bacterial counts on the order of 10^5 (Cancian 1988). Similarly, water in the Timavo Fishpond Cave shows elevated chloride and sulfate chemistry, higher than any of the other surrounding groundwaters (Gemiti 1994). Based on the water chemistries of these and other water table caves in the vicinity of the Timavo springs, Gemiti (1994) concluded that a shallow hydrologic regime exists that is independent of the Timavo conduit network. It seems likely that this circulation occurs within the epikarst, and that an anthropogenic source of pollution affects the chemistry of these cave waters.

Methods

Water sampling

In order to determine the sources of water contributing to the Klariči supply, high frequency water sampling was conducted at the monitoring well B-4 prior to and during the autumn wet seasons of 1999 and 2000. In 1999, water samples from well B-4 were collected up to four times per day (at minimum once per day) for a period of 5 weeks,

Table 2 Data from well B-4 during 1999 storm events used for the PCA model

Date/time	Cl (mg/L)	Ca (mg/L)	Mg (mg/L)	$\delta^{18}O$ ‰ (VSMOW)[a]
10/16/99 4:00	28.0	60.5	11.2	−7.66
10/17/99 4:00	24.7	58.9	10.7	−7.72
10/18/99 4:00	25.2	58.9	11.2	−7.64
10/23/99 16:00	20.0	58.5	10.2	−7.81
10/24/99 16:00	25.7	62.1	10.7	−7.79
10/24/99 22:00	31.4	65.3	10.9	−7.75
10/25/99 4:00	35.2	71.3	10.7	−7.51
10/25/99 16:00	33.3	73.3	10.5	−6.90
10/26/99 4:00	31.4	77.0	10.1	−7.21
10/26/99 16:00	34.2	76.2	10.7	−6.98
10/27/99 4:00	32.8	75.4	11.2	−7.35
10/27/99 16:00	35.2	76.0	9.6	−7.34
10/28/99 4:00	34.2	73.7	11.2	−7.10
10/28/99 16:00	35.2	73.9	11.9	−6.92
10/29/99 4:00	35.6	72.7	10.8	−7.04
10/29/99 16:00	38.0	73.3	10.8	−7.09
10/30/99 4:00	38.0	73.3	10.5	−7.00
10/30/99 16:00	36.1	72.9	10.5	−7.18
10/31/99 4:00	30.4	73.1	10.6	−7.10
10/31/99 16:00	40.4	72.1	11.1	−6.90
11/1/99 4:00	35.6	70.3	10.8	−6.57
11/3/99 16:00	32.3	66.9	11.3	−7.36
11/4/99 16:00	31.8	65.7	11.4	−7.42
11/7/99 16:00	29.9	64.3	11.2	−7.55
11/9/99 16:00	32.8	66.1	10.7	−7.57

[a] *VSMOW* Vienna Standard Mean Ocean Water

 DOI 10.1007/s10040-006-0031-6

Table 3 Data from 2000 storm event sampling at well B-4

Sample #	Date/time	Precip. (mm)	EC (μS/cm)	pH	Temp. (°C)	Cl (mg/L)	Ca (mg/L)	Mg (mg/L)	DIC (mgC/L)	$ePCO_2$	δ^{13}C-DIC ‰ (VPDB)[a]	δ^{18}O ‰ (VSMOW)[b]	δ^{2}H ‰ (VSMOW)[b]
1	9/28/00 7:00		428	7.43	14.5	25.1	47.5	9.2	16.9	8.8	−11.2	−7.68	−48.7
2	9/29/00 7:00	35.4	431	7.56	14.6	24.0	46.5	9.2	17.7	7.0	−11.1	−7.77	−47.9
3	9/30/00 7:00	66.8	397	7.49	14.6	24.0	46.9	9.3	16.1	7.4	−11.0	−7.68	−48.2
4	9/30/00 15:00		431	7.51	14.8	24.5	49.0	9.1	16.1	7.1	−10.8	−7.90	−48.0
5	9/30/00 23:00		431	7.44	14.5	24.5	45.5	9.5	16.9	8.6	−11.2	−7.73	−48.1
6	10/1/00 7:00	4.6	426	7.50	15.0	24.0	46.5	9.0	16.7	7.5	−11.2	−7.82	−47.3
7	10/1/00 15:00		437	7.59	14.6	26.0	44.5	9.4	16.4	6.1	−11.4	−7.89	−49.5
8	10/1/00 23:00		459	7.40	15.0	26.6	54.2	9.0	17.4	9.7	−12.0	−7.51	−48.2
9	10/2/00 7:00	2.3	494	7.30	14.7	26.1	70.5	7.7	19.8	13.5	−12.3	−7.12	−46.4
10	10/2/00 15:00		495	7.32	15.0	24.5	49.5	6.5	25.0	16.4	−12.6	−6.93	−44.0
11	10/2/00 23:00		484	7.19	14.9	21.0	80.2	6.2	27.1	23.0	−12.8	−6.84	−43.0
12	10/3/00 7:00		522	7.15	14.8	18.0	49.5	6.0	27.3	25.1	−13.0	−6.87	−43.7
13	10/3/00 15:00		499	7.22	14.7	18.0	65.2	6.1	27.6	22.1	−12.7	−6.90	−43.8
14	10/3/00 23:00		501	7.19	14.9	18.5	75.9	6.4	26.8	22.8	−12.9	−6.88	−44.4
15	10/4/00 7:00		488	7.18	14.6	20.0	55.5	6.5	26.3	22.7	−13.0	−6.85	−44.8
16	10/4/00 15:00		515	7.22	14.8	23.0	49.2	6.8	26.5	21.3	−13.1	−6.91	−44.5
17	10/4/00 23:00		521	7.22	14.8	26.6	52.8	7.0	26.3	21.1	−13.0	−6.89	−44.8
18	10/5/00 8:00	4.9	525	7.13	15.0	27.1	79.3	7.4	25.8	24.7	−12.7	−6.81	−44.0
19	10/5/00 16:00		550	7.29	15.1	35.6	58.6	7.9	26.0	18.2	−12.7	−7.09	−44.4
20	10/5/00 23:00		580	7.25	15.0	37.1	79.7	8.4	25.2	19.1	−12.5	−7.01	−46.2
21	10/6/00 7:00		567	7.28	15.1	37.6	64.7	8.4	24.5	17.5	−12.8	−7.02	−45.5
22	10/6/00 15:00		570	7.40	14.8	40.1	68.3	8.6	25.0	13.9	−12.7	−7.05	−46.1
23	10/6/00 23:00		583	7.23	14.8	43.6	65.8	9.0	23.9	18.8	−12.5	−7.04	−45.0
24	10/7/00 7:00		586	7.20	14.9	43.6	69.2	8.8	25.2	21.1	−12.7	−7.03	−44.7
25	10/7/00 15:00		605	7.15	15.0	47.1	72.0	9.2	24.7	22.8	−12.8	−7.03	−46.0
26	10/7/00 23:00		593	7.24	14.3	47.1	69.8	9.3	22.6	17.3	−12.4	−7.10	−43.0
27	10/8/00 7:00	4.2	586	7.29	14.4	47.6	73.3	9.2	22.9	15.8	−12.2	−7.08	−44.6
28	10/8/00 15:00		591	7.34	14.3	49.1	75.6	9.4	23.7	14.8	−12.2	−7.13	−44.9
29	10/8/00 23:00		596	7.31	14.3	50.1	76.6	9.5	22.9	15.2	−12.2	−7.11	−44.9
30	10/9/00 7:00	29.1	574	7.26	14.3	45.1	70.3	9.4	21.9	16.0	−12.3	−7.22	−45.3
31	10/9/00 15:00		554	7.43	14.3	45.1	68.0	9.9	21.9	11.3	−12.1	−7.21	−43.6
32	10/9/00 23:00		540	7.34	14.2	45.1	66.2	9.4	22.1	13.8	−12.2	−7.26	−45.7
33	10/10/00 7:00	2.2	544	7.35	14.1	46.6	69.2	9.7	22.6	13.8	−12.1	−7.24	−46.3
34	10/10/00 15:00		579	7.35	14.2	48.1	72.1	9.7	23.2	14.1	−12.2	−7.14	−44.8
35	10/10/00 23:00		568	7.31	14.2	45.1	67.0	9.6	22.6	15.0	−12.1	−7.24	−46.7
36	10/11/00 7:00		520	7.29	14.3	37.1	62.8	9.1	21.6	14.9	−11.9	−7.37	−45.8
37	10/11/00 15:00		521	7.44	14.5	36.6	63.5	9.1	21.6	11.0	−12.0	−7.30	−45.5
38	10/11/00 23:00		536	7.34	14.3	36.6	65.6	9.1	21.9	13.6	−12.2	−7.31	−46.5
39	10/12/00 7:00		547	7.29	14.5	38.1	67.0	8.8	23.7	16.4	−12.4	−7.22	−45.3
40	10/12/00 15:00		565	7.30	14.4	37.6	67.3	8.7	23.9	16.2	−12.7	−7.11	−44.3
41	10/12/00 23:00		566	7.28	14.6	35.1	56.9	8.1	26.3	18.6	−12.7	−7.03	−45.1
42	10/13/00 7:00		555	7.26	14.6	33.1	56.6	7.9	25.0	18.4	−13.0	−7.06	−43.3
43	10/14/00 7:00	16.5	549	7.30	14.7	30.6	46.0	7.6	25.2	17.2	−13.3	−6.97	−44.1
44	10/14/00 15:00			7.32	14.7	30.6	45.1	7.6	26.3	17.2	−13.2	−6.99	−44.9
45	10/15/00 7:00	9.6	547	7.25	15.1	30.6	61.3	7.7	24.5	18.5	−13.2	−7.07	−45.0
46	10/16/00 7:00		549	7.18	15.1	33.1	45.7	8.0	26.0	22.7	−13.3	−7.10	−43.2
47	10/17/00 7:00		553	7.30	14.7	35.1	58.2	8.6	24.2	16.5	−13.0	−7.14	−43.3
48	10/18/00 7:00		558	7.35	14.5	34.1	51.4	9.0	22.4	13.7	−12.7	−7.18	−45.1
49	10/19/00 7:00		562	7.27	14.7	42.6	66.3	9.1	23.2	16.8	−13.8	−7.27	−44.6

DOI 10.1007/s10040-006-0031-6

Table 3 (continued)

Sample #	Date/time	Precip. (mm)	EC (µS/cm)	pH	Temp. (°C)	Cl (mg/L)	Ca (mg/L)	Mg (mg/L)	DIC (mgC/L)	$ePCO_2$	δ^{13}C- DIC ‰ (VPDB)[a]	δ^{18}O ‰ (VSMOW)[b]	δ^{2}H ‰ (VSMOW)[b]
50	10/20/00 7:00		564	7.33	14.5	43.6	60.5	9.2	21.1	13.5	−12.1	−7.22	−43.8
51	10/21/00 7:00		556	7.40	14.3	42.1	58.5	9.3	23.2	12.8	−13.2	−7.29	−43.5
52	10/22/00 7:00			7.45	14.1	42.1	62.8	9.6	21.3	10.6	−12.9	−7.35	−45.3
53	10/23/00 7:00		542	7.34	14.2	41.1	55.7	9.3	23.2	14.4	−13.1	−7.45	−45.3
54	10/24/00 7:00		526	7.44	14.1	41.1	55.1	9.4	20.8	10.5	−13.4	−7.58	−46.5
55	10/25/00 7:00		520	7.42	14.3	39.1	51.4	9.3	20.8	11.0	−13.0	−7.55	−48.9
56	10/26/00 7:00		505	7.40	14.3	40.6	54.8	9.8	20.8	11.5	−12.8	−7.56	−47.4
57	10/27/00 7:00		523	7.37	14.3	39.6	51.0	9.6	20.6	12.1	−12.8	−7.54	−47.9
58	10/28/00 7:00		520	7.40	14.1	40.6	49.4	9.9	20.3	11.1	−12.8	−7.56	−49.3
59	10/29/00 7:00	2.1	498	7.40	14.2	35.1	45.2	9.5	20.3	11.2	−12.4	−7.63	−50.0
60	10/30/00 7:00	38.0	505	7.42	14.1	36.6	45.2	9.7	20.3	10.7	−12.7	−7.65	−50.2
61	10/31/00 7:00		505	7.37	14.4	36.6	51.7	9.6	17.4	10.2	−11.2	−7.66	−49.6
62	11/1/00 7:00	22.1	505	7.39	14.5	37.6	50.9	9.7	18.2	10.3	−11.1	−7.68	−49.1
63	11/2/00 7:00	59.8	474	7.45	14.1	30.1	44.8	9.4	16.7	8.2	−11.2	−7.79	−50.9
64	11/3/00 7:00	0.2	522	7.39	14.2	37.1	53.3	9.4				−7.67	−47.6
65	11/4/00 7:00	2.4	532	7.28	14.3	31.6	51.4	8.0				−7.23	−46.0
66	11/5/00 7:00		552	7.18	14.0	17.5	75.9	5.9				−6.93	−43.7
67	11/7/00 7:00		550	7.19	14.1	21.5	60.6	6.3				−6.90	−42.8

[a] *VPDB* Vienna Pee Dee Belemnite

[b] *VSMOW* Vienna Standard Mean Ocean Water

from September 19 to November 16 1999. In 2000, samples were collected from 26 September to 7 November three times per day during the first week, after which the sampling frequency was decreased to once per day for the remaining three weeks of sampling. Water samples were collected from the Soča River at Mainizza (Fig. 2) and from well B-3 on a monthly basis between 1999 and 2000, as well as during the storm events (Doctor 2002).

Measurements of pH, temperature, and electrical conductivity (EC) were taken in the field. In addition, a datalogger with a conductivity/temperature probe was placed inside monitoring well B-4 during the storm event sampling of 2000, with measurements taken every 15 min. Although water sample collection ended before the largest flood event occurred, the EC probe was left inside of the well after sampling ceased, and continued to collect data for another 2 months. Thus, a much longer record of EC at well B-4 during the record-breaking rainfall of 2000 is available.

Water samples were analyzed for ionic concentrations of Ca^{2+}, Mg^{2+}, and Cl^{-}. Ca^{2+} and Mg^{2+} concentrations were determined by flame atomic absorption spectroscopy (AAS) at the Jožef Stefan Institute in Ljubljana, Slovenia. Cl^{-} concentrations were measured colorimetrically at the Karst Research Institute in Postojna, Slovenia. Water stable isotope compositions ($\delta^{18}O$, $\delta^{2}H$) were determined at the Institute for Hydrology, Neuherberg, Germany. $\delta^{18}O$ measurements were made by the CO_2 equilibration method (Epstein and Mayeda 1953) with 1σ precision of ±0.1‰. $\delta^{2}H$ measurements were made by the Cr-reduction method (Gehre et al. 1996) with 1σ precision of ±1.0‰. Both $\delta^{2}H$ and $\delta^{18}O$ measurements were normalized to the Vienna Standard Mean Ocean Water (VSMOW) scale.

For water resource management in karst areas, it is important to quantify contributions to water supplies from the shallow epikarst zone. For this purpose, the $^{12}C/^{13}C$ ratio of dissolved inorganic carbon (DIC) is a particularly useful natural tracer in conjunction with water isotopes and major ion chemistry (Doctor et al. 2000; Lee and Krothe 2001; Emblanch et al. 2003; Desmarais and Rojstaczer 2002). Samples for $\delta^{13}C_{DIC}$ were collected by filtering 15 ml of water through 0.45-µm filters with a syringe into vials containing 50 µl of saturated $HgCl_2$ preservative. The vials were immediately closed without headspace with open-top septa caps using low-diffusion butyl rubber septa, and stored chilled until analysis. $\delta^{13}C_{DIC}$ measurements were made at the Jožef Stefan Institute in Ljubljana, Slovenia following a procedure modified from Mook et al. (1974). For the CO_2 extraction, 5 ml of a water sample were removed from a sample vial with a syringe, and injected into closed evacuated glass vessels containing approximately 0.5 ml of concentrated phosphoric acid (100% H_3PO_4). The exsolved CO_2 was quantitatively frozen into an evacuated Exetainer vial cooled with liquid nitrogen, and the resulting gas was analyzed with a Europa Scientific ANCA 20-20 mass spectrometer (use of trade names is for identification purposes only and does not imply endorsement by the U.S. Government). The $\delta^{13}C_{DIC}$ measurements were

DOI 10.1007/s10040-006-0031-6

normalized to the Vienna Pee Dee Belemnite scale (VPDB) and 1σ precision of duplicate analyses was within ±0.3‰. Total DIC concentrations were determined by integration of the total ion count from the mass spectrometer referenced against known quantities of CO_2 gas. Calculations of the partial pressure of CO_2 (PCO_2) and saturation index of calcite (SI_{calc}) were conducted using the geochemical speciation program PHREEQC (Parkhurst and Appelo 1999).

PCA and EMMA

A water sample taken from a stream, spring or well normally represents a mixture of water from different sources which combine to give the measured chemistry of the sample. If these distinct source solutions are considered as end members (i.e., their chemical compositions are extreme in relation to the mixture), it is possible to define a system of simple linear equations by which to calculate mixing proportions between these water sources. Such a model for end-member mixing analysis (EMMA) that utilizes the statistical factors generated through principal components analysis (PCA) was outlined by Christophersen and Hooper (1992).

PCA is a statistical technique used for multivariate data reduction while retaining those characteristics of the dataset that contribute most to its variance (Reyment and Jöreskog 1993). Several studies reported in the literature illustrate applications of PCA for interpreting hydrologic processes from the analysis of large hydrogeochemical data sets (e.g., Melloul and Collin 1992; Lastennet and Mudry 1997; Laaksoharju et al. 1999; Andreo and Carrasco 1999; Burns et al. 2001; Stetzenbach et al. 2001). In this study, PCA was applied to identify the most important statistical factors contained within the chemical and isotopic data generated. These factors were then used to estimate mixing proportions between the water sources that contribute to the karst aquifer discharge.

For data that exhibit strong correlations among variables, typically only the first few principal components will account for the majority of the variance of the dataset. A common criterion for determining the number of components to retain for further analysis is those having an eigenvalue greater than 1. However, in the case of determining source solution end members that mix together and give rise to the observed values in the water samples, the number of retained principal components, n_c, necessitates n_c+1 end members. Therefore, one must judge how many components to retain based on the system being studied, and whether additional end members are justified. The choice of the number of end members to retain for the EMMA is arbitrary; however, the goal is to maximize the cumulative amount of data variance that can be explained via a minimum number of principal components retained.

The chemical and isotopic parameters considered in this analysis each have distinct scales and variances, therefore the data are first standardized according to the formula:

$$z_{ij} = \frac{x_{ij} - \bar{x}_j}{s_j} \quad (1)$$

where x_{ij} is the raw value of chemical parameter j in the sample or observation i, $\bar{x}_j$ is the mean value of parameter x_j for all of the samples, and s_j is the standard deviation of parameter x_j for all the samples. Once the data are standardized, the PCA can be performed using a commercially available statistical software package. The software utilized for the PCA calculations in this study was SPSS version 11.0.1 (SPSS Inc. USA 2001). The EMMA model is available from the US Geological Survey as a Microsoft Excel spreadsheet.

Results

The data obtained from the analysis of water samples from well B-4 and used in the PCA model for 1999 and 2000 are provided in Table 2 and Table 3, respectively.

Storm events and chemographs

During sampling in October of 1999, 76 mm of rain fell over the course of 7 days, with one storm dropping 35 mm of rain in less than 24 h. This event had been preceded by 2 weeks without rainfall, however several large rain events had occurred in September 1999, prior to the event sampling. In 2000, three storm events occurred during the sampling period. The first storm in 2000 brought 109 mm of rainfall from 29 September to 2 October. This rain event was preceded by more than 3 weeks without measurable rainfall. A second storm then truncated the recession from the first event, and 35 mm of rain fell from 8–10 October 2000. Finally, from 29 October to 4 November 2000, 125 mm of rain fell, again truncating the recession of the previous rain event. Immediately after sampling in 2000 ended, record rainfall occurred across Slovenia spawning a 100-year flood event in some areas. The total rainfall amount from 1 October to 31 December 2000 measured at the Sela na Krasu precipitation gauging station less than 4 km from the Klariči pumping station equaled 923 mm, more than twice the autumn season average rainfall amount for the region (30-year mean from 1960–1990) of 454 mm. In the most extreme event of 2000, 157 mm of rain fell at Sela na Krasu during a single storm on November 19.

The chemographs obtained during the storm sampling at well B-4 during 1999 are shown in Fig. 3, and the chemographs obtained for the storm sampling during 2000 are shown in Fig. 4. Figure 4a shows the parameters used in the PCA/EMMA modeling described later. Figure 4b shows the $\delta^{13}C_{DIC}$ values of the well in time series along

 DOI 10.1007/s10040-006-0031-6

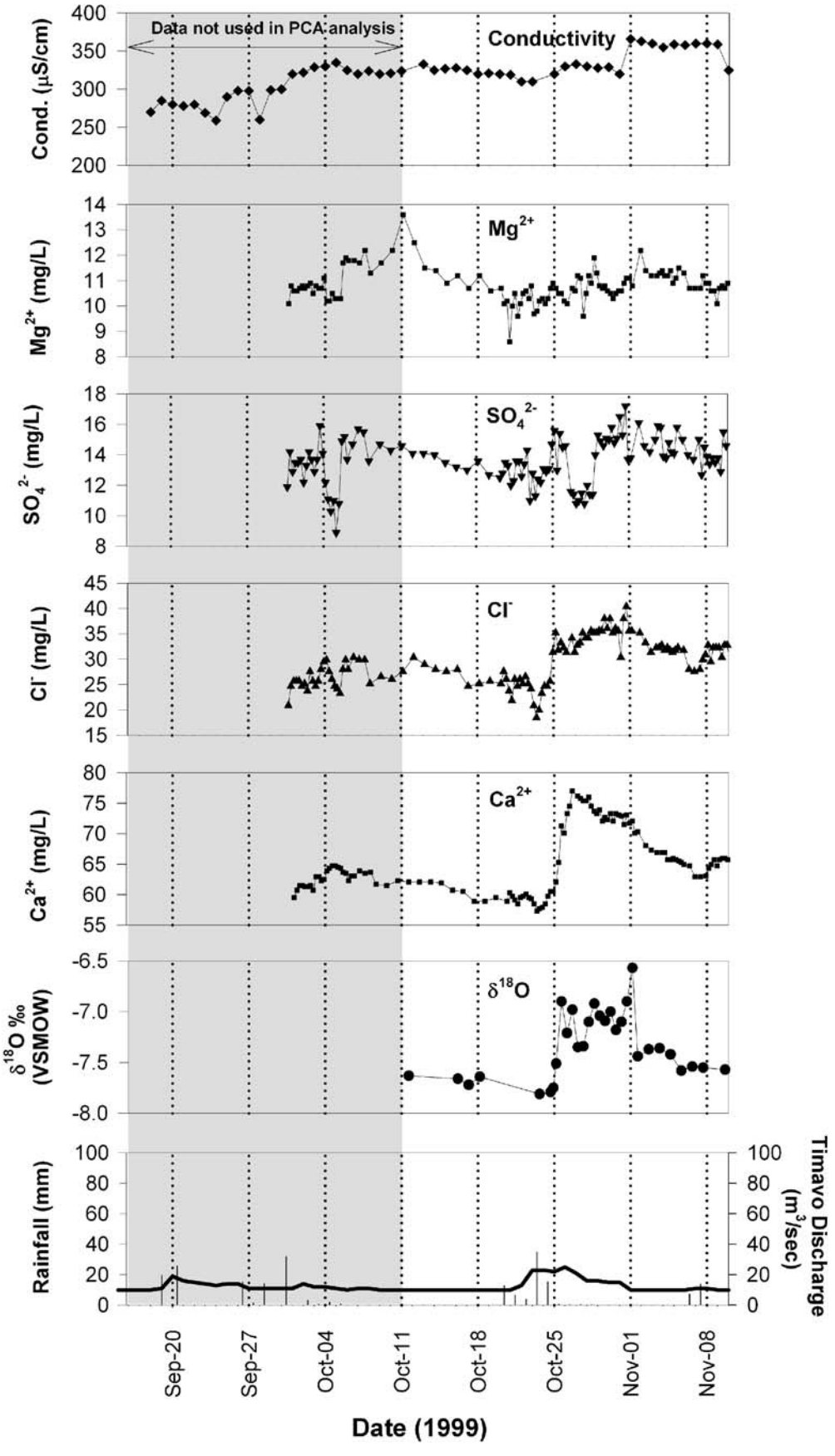

Fig. 3 Chemical and isotopic chemographs from well B-4 for the parameters used in the PCA from the storm events in 1999

DOI 10.1007/s10040-006-0031-6

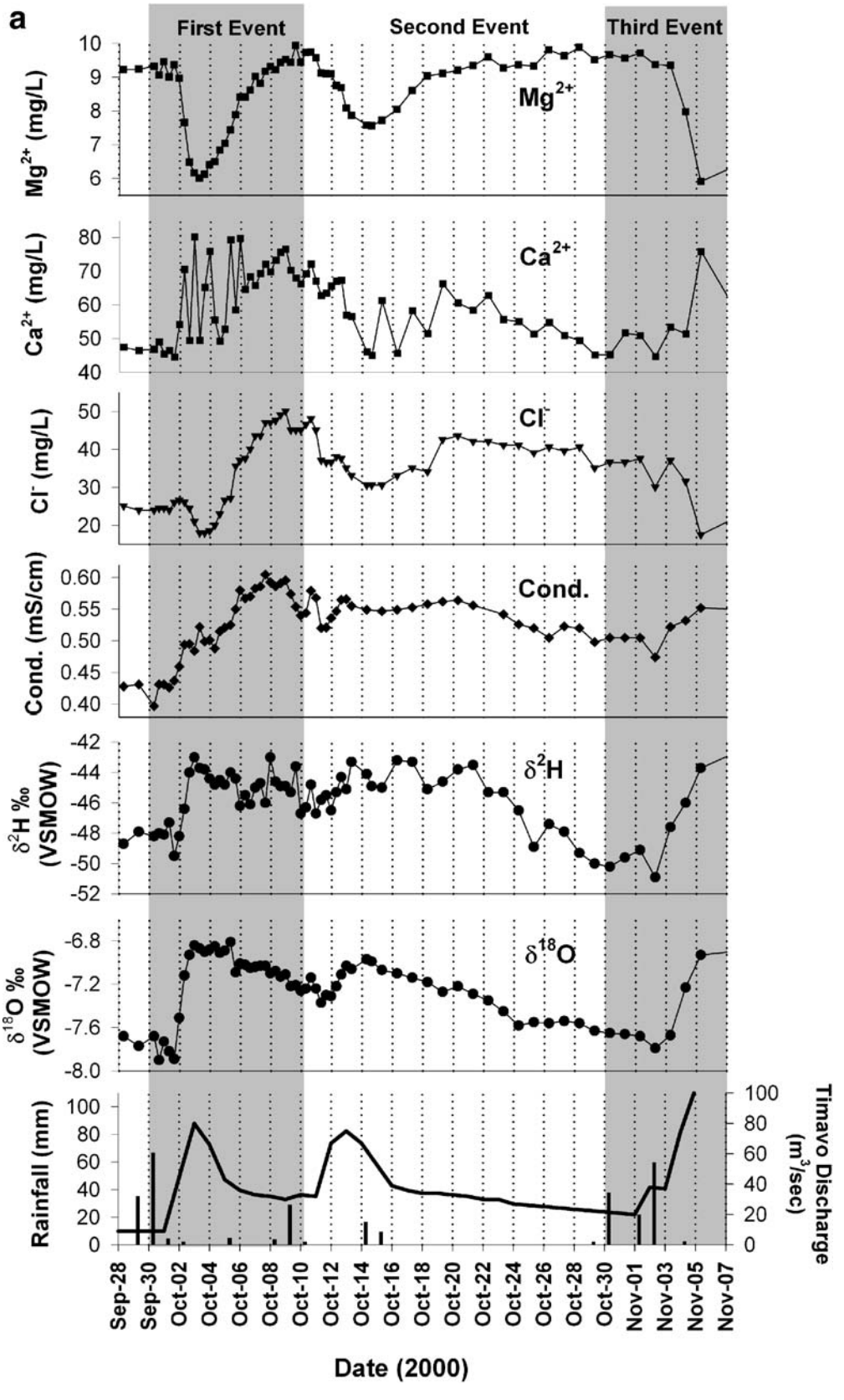

Fig. 4 **a** Chemical and isotopic chemographs from well B-4 during the storm events in 2000. **b** Additional chemical and isotopic chemographs from well B-4 during the storm events in 2000

with total DIC concentrations, field pH and temperature measurements, calculated excess PCO_2 (or $ePCO_2$, equivalent to the ratio of the PCO_2 of the solution to that in the atmosphere), and saturation index of calcite (SI_c). Water levels in well B-4 were not measured during the events; instead, the discharge of the Timavo springs is provided as

 DOI 10.1007/s10040-006-0031-6

Fig. 4 (continued)

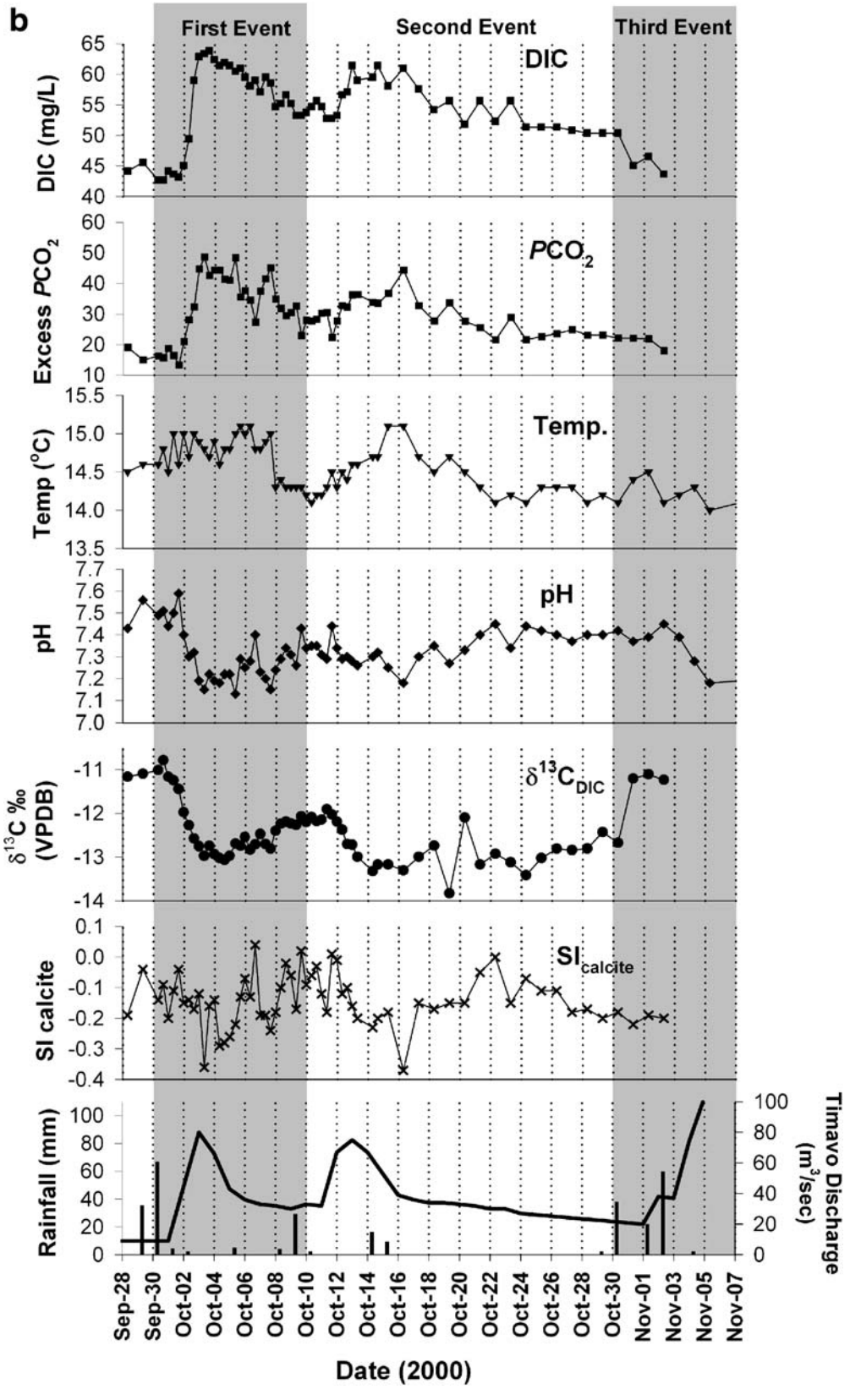

DOI 10.1007/s10040-006-0031-6

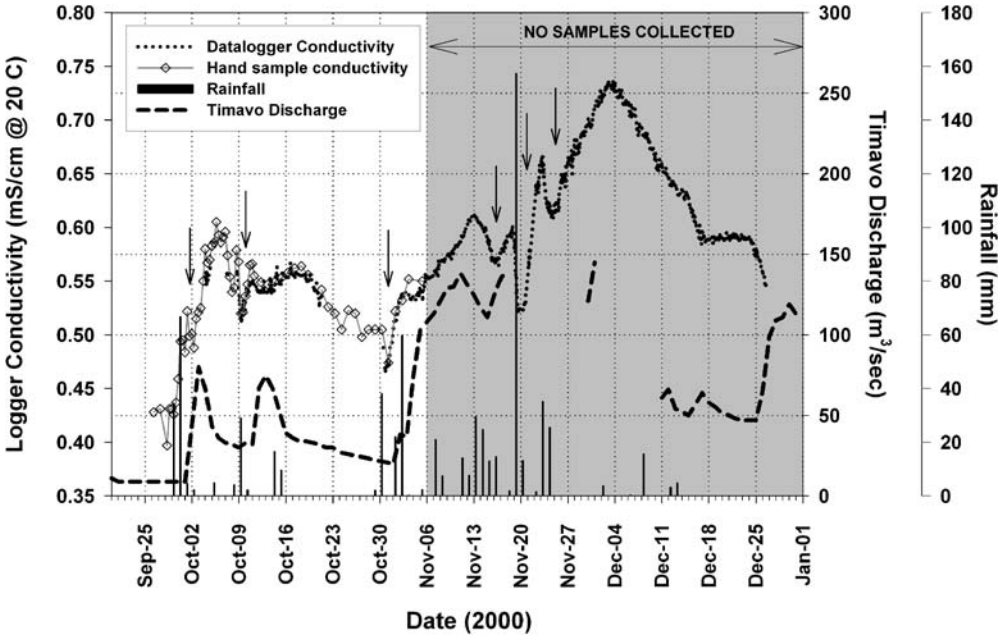

Fig. 5 Conductivity measured at well B-4 in 2000. The *open diamonds* show the period of hand-sampling during which all other chemical and isotopic parameters were measured. The *dotted line* shows the continuous record of conductivity as measured by the datalogger. The *dashed line* is the discharge of the Timavo springs, plotted as a proxy for the regional hydraulic head response to the storm events. *Arrows* indicate large rainfall events that caused short-lived dilution of the conductivity signal. Rainfall was measured at the Sela na Krasu precipitation station

a proxy for changes in the regional head during the storms. With the onset of rainfall, several stages in the chemical evolution of the well water take place. This pattern is marked by:

1. Increases in Ca^{2+} and specific conductivity following rainfall, except after the most extreme rainfall events in which the conductivity decreased for a short duration
2. Positive shifts in $\delta^{18}O$ immediately following rainfall, irrespective of the $\delta^{18}O$ composition of the rainfall
3. A decrease in Mg^{2+} concentrations immediately following rainfall
4. An initial rapid decrease in Cl^- followed by an increase in Cl^- concentrations to levels greater than those prior to the event
5. Depletion in $\delta^{13}C_{DIC}$ composition on the rising limb of an event followed by increasing values on the recession limb
6. A return toward the pre-storm chemical and isotopic compositions during storm recession in all of the measured parameters, but most gradual in the conductivity values

Figure 5 shows the continuous conductivity data recorded at well B-4, with hand-sample measurements plotted along with the datalogger record for comparison. During the period of sample collection, the datalogger record matches with the hand-sample measurements, providing a nearly continuous record of conductivity over the monitoring period. The gaps in the datalogger record are due to water levels in the well being just lower than the probe, such that the probe was not fully submerged. With

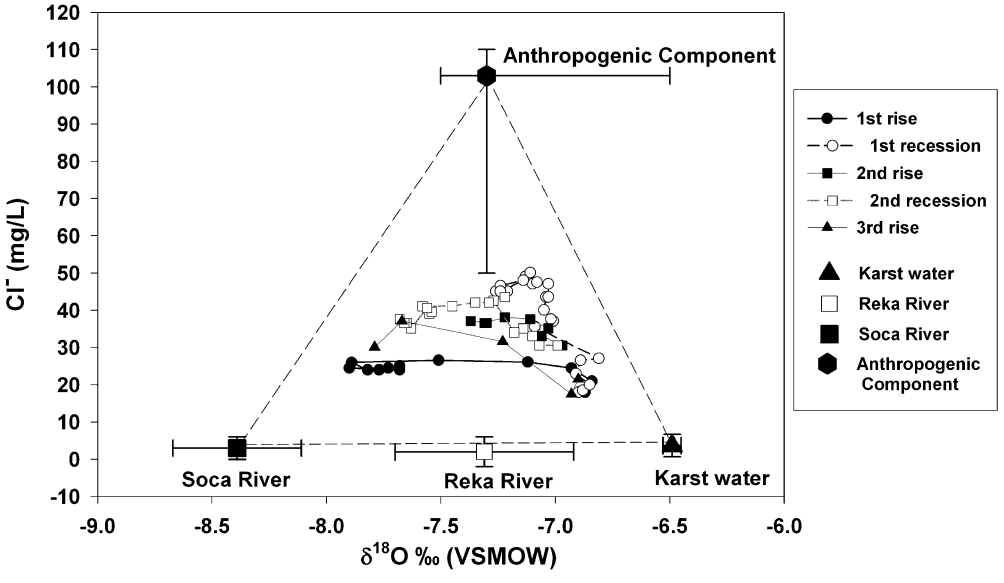

Fig. 6 Representative bivariate plot showing the end members and the composition of well B-4 measured during the storm events of 2000. Note the evolution of the well water during successive events moving first from Soča River composition toward the karst water, then toward the anthropogenic component on the recession limb

 DOI 10.1007/s10040-006-0031-6

Table 4 End members for PCA/EMMA analysis of storm event sampling at well B-4

End member	Year	Mg (mg/L)	Ca (mg/L)	Cl (mg/L)	EC (μS/cm)	$\delta^{18}O$ ‰ (VSMOW)	$\delta^{13}C$ ‰ (VPDB)
Karst water	2000	2.6	108	3.7	560	−6.5	−13.8
	1999	2.6	108	3.7	–	−6.5	–
Anthropogenic component	2000	16	124	103	815	−7.30[a]	−14.0[a]
	1999	16	124	103	–	−7.30	–
Soča River	2000	8.4	41.9	3.0	268	−8.39	− 9.34
	1999	9.5	41.9	3.0	–	−8.39	

[a] Estimated from bi-variate plots

continued rainfall, however, the water table rose, and the probe remained fully submerged from the time just prior to the termination of sample collection up until the probe was removed from the well. After sampling had ended, the EC of the well water progressively increased with greater amounts of rainfall during the flood of November 2000 (Fig. 5). However, the general gradual increase is punctuated by dilution caused by the largest rainfall events. These dilution signals are short-lived (1–2 days) and are consistently followed by EC values greater than what had preceded each event.

Bi-variate mixing plots

Bi-variate plots were constructed for the chemical and isotopic data collected during both the monthly sampling and storm sampling to explore mixing trends. A representative bi-variate plot of the most conservative tracers (Cl^- and $\delta^{18}O$) during storm event sampling at well B-4 is shown in Fig. 6. It is not possible to account for the distribution of samples shown in Fig. 6 with a model of mixing between solely two end members; however, the data can be completely enclosed by a model employing three end members.

End members

On the basis of the data from the bi-variate plots, the following three end members were chosen for the EMMA model:

1. Soča River water (allogenic recharge)
2. Water from well B-3 (autogenic recharge)
3. Timavo Fishpond Cave water (anthropogenic component)

The chemical and isotopic compositions of two of these water sources, the well B-3 (representing local autogenic recharge to the aquifer) and the Soča River (representing allogenic recharge to the aquifer), were repeatedly determined over a period of 2 years and appear to mix and give rise to the majority of springs and water table caves in the Kras resurgence zone (Doctor 2002; Doctor and Alexander 2005). The Soča River end member is represented by the mean annual composition of the river. Water from well B-3 is the typical "karst water" first described by Gemiti and Licciardello (1977) which arises from autogenic recharge and chemical reaction with the soil and host rock. The third end member was not directly sampled during this study; however, its composition has been inferred from the singular measured chemistry of the Timavo Fishpond Cave. While this composition may reflect a mixture of sources itself, its chemical signature is sufficiently extreme in relation to the mixture observed at the water supply well to make it a viable end-member choice. Due to the elevated levels of chloride and sulfate and lack of seawater influence observed in this water (Cancian 1987), it is assumed to be impacted by anthropogenic activities. The compositions of the three end members used for the mixing analysis are shown in Table 4.

PCA/EMMA results

The data were standardized according to Eq. 1, and the PCA was performed on the correlation matrix of the

Table 5 Results of the PCA from 2000 and 1999 at well B-4

	Principal component	Ca	Mg	Cl	$\delta^{18}O$	EC	$\delta^{13}C_{DIC}$	Cumulative variance explained
2000 Storm samples								
	PC 1	−0.438	0.171	−0.269	−0.504	−0.520	0.427	49.0%
	PC 2	−0.114	−0.654	−0.605	0.304	−0.256	−0.188	83.7%
	PC 3	0.699	−0.088	−0.114	0.141	−0.144	0.671	95.8%
	PC 4	−0.540	−0.160	0.106	0.390	0.439	0.571	99.0%
	PC 5	0.121	−0.344	−0.255	−0.661	0.602	0.054	99.6%
	PC 6	−0.027	−0.626	0.687	−0.211	−0.297	0.044	100.0%
1999 Storm samples								
	PC 1	−0.583	0.033	−0.578	−0.570	–	–	63.4%
	PC 2	−0.176	0.970	0.122	0.112	–	–	89.6%
	PC 3	−0.196	−0.053	−0.581	0.788	–	–	95.9%
	PC 4	0.769	0.233	−0.559	−0.205	–	–	100.0%

 DOI 10.1007/s10040-006-0031-6

standardized data set. For the data from 2000, the first two principal components accounted for the majority of the variance of the data set from 2000 (83.7%), with little significant contribution from the remaining four components (Table 5). Similarly, the PCA results from the 1999 data show 89.6% of the variance explained by the first two principal components (Table 5). Retaining two components necessitates mixing between three end members; thus, a mixing model employing the three hypothesized end members is justified.

The EMMA model was used to calculate mixing proportions in the well water samples derived from the three hypothesized end members by solving the following linear mass-balance equations:

$$1 = p_{\mathrm{Karst}} + p_{\mathrm{Soca}} + p_{\mathrm{Anth}} \tag{2}$$

$$U1_{\mathrm{Sample}} = p_{\mathrm{Karst}} \bullet (U1_{\mathrm{Karst}}) + p_{\mathrm{Soca}} \bullet (U1_{\mathrm{Soca}}) + p_{\mathrm{Anth}} \bullet (U1_{\mathrm{Anth}}) \tag{3}$$

$$U2_{\mathrm{Sample}} = p_{\mathrm{Karst}} \bullet (U2_{\mathrm{Karst}}) + p_{\mathrm{Soca}} \bullet (U2_{\mathrm{Soca}}) + p_{\mathrm{Anth}} \bullet (U2_{\mathrm{Anth}}) \tag{4}$$

where p is the proportion of each end member in the water sample, and $U1$ and $U2$ are the values of the first and second principal component for each observed sample and the end-member compositions projected into two-dimensional mixing space. The subscripts Karst, Soca, and Anth signify the three end-members: karst water, Soča River, and anthropogenic component, respectively. Equation 2 constrains the proportions of the three end members to sum to 1 in each well-water sample.

The two principal components retained form the axes of a two-dimensional space (hereafter referred to as U-space after the terminology of Christophersen and Hooper 1992) into which the standardized spring or well water samples and end members were projected (Fig. 7). The projected values are obtained by a matrix multiplication of the eigenvectors and the standardized sample values. In the case of the end members, they are standardized according to the mean and standard deviations of the sample data, so as to be plotted on the same axes in U-space. The three end-member compositions, when also projected into U-space, form the corners of a triangle within which should fall the observations if each observation is a mixture of the three end members. If an observation falls outside the limits of the triangle, it is orthogonally projected onto the closest line of the triangle. In that case, the observation is assumed to be a linear mixture of only two of the end members.

The EMMA analysis for this study was performed twice: once on the water samples collected in 1999, and once for those collected in 2000. For the analysis of the

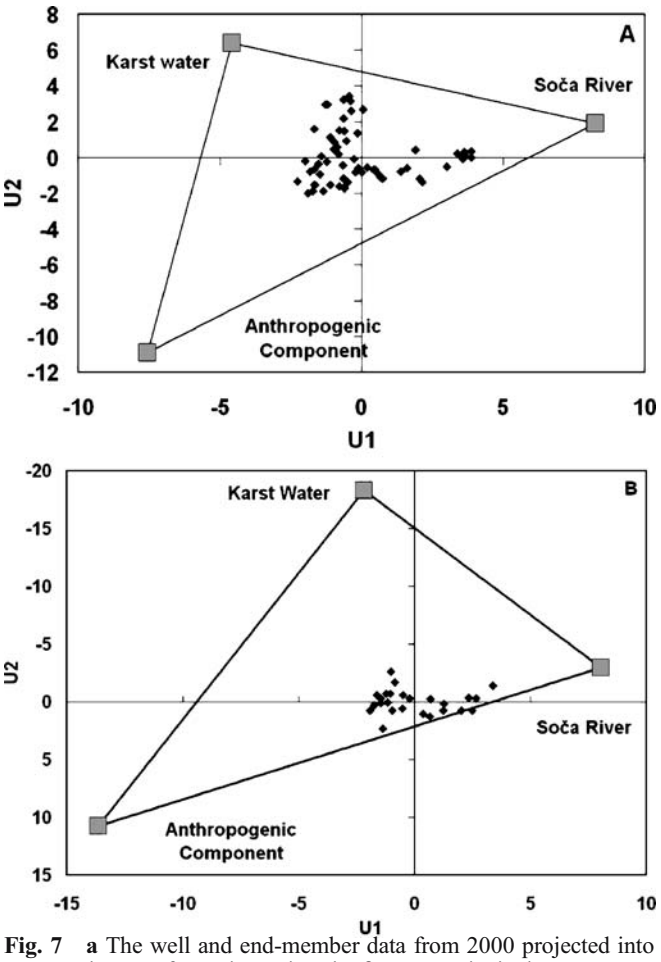

Fig. 7 **a** The well and end-member data from 2000 projected into U-space by transformation using the first two principal components of the 6-parameter principal components analysis. **b** The well and end-member data from 1999 projected into U-space by transformation using the first two principal components of the 4-parameter principal components analysis

2000 samples, six parameters were used: Mg^{2+}, Ca^{2+}, Cl^{-}, EC, $\delta^{18}O$, and $\delta^{13}C_{DIC}$. For the analysis of the 1999 samples, $\delta^{13}C_{DIC}$ measurements were not available and EC data were collected with a different instrument, thus only four parameters were used: Mg^{2+}, Ca^{2+}, Cl^{-}, and $\delta^{18}O$. The results from 2000 projected into U-space are shown in Fig. 7a, and those from 1999 are shown in Fig. 7b. These plots show that the data are well circumscribed by the three end members described earlier, lending further support to the choice of the hypothesized end members.

The calculated proportions of the three end members in each observed sample from well B-4 in 2000 are shown in Fig. 8a, and results from 1999 are shown in Fig. 8b. In Fig. 8a, two storm events from 2000 are represented, the recession of the first having been truncated by the second storm event. The proportions of the three end members contributing to the well discharge were summed across each of the two complete storm events (the event that began 29 October 2000 was omitted because only the rising limb was sampled). These results are presented in Table 6.

 DOI 10.1007/s10040-006-0031-6

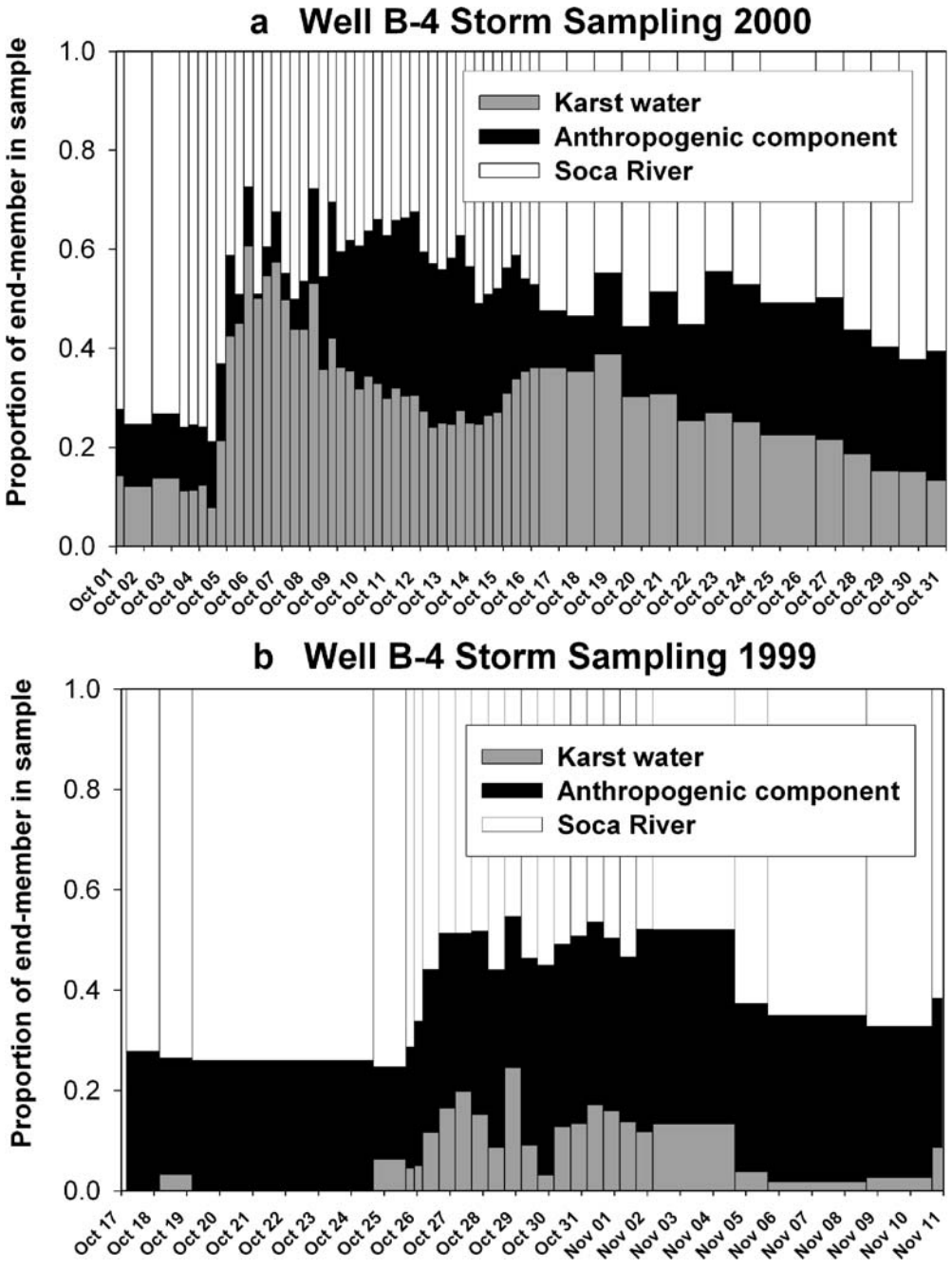

Fig. 8 The calculated proportions of each end member in a sample for every sample collected during the storm events of **a** 2000 and **b** 1999. Note the higher proportion of the anthropogenic end member in 1999 when antecedent conditions were wetter than in 2000

Table 6 Total end-member proportions estimated at the Klariči well (B-4) in 1999 and 2000

End member	Storm event 1999	First storm event 2000	Second storm event 2000
Soča River	58%	41% (47%)[a]	43% (54%)
Karst water	10%	34% (32%)	29% (24%)
Anthropogenic component	32%	25% (21%)	28% (22%)

[a] Values in parentheses represent the data analysis performed on the 2000 storm data with the 4 parameters Ca, Mg, Cl and δ^{18}O only

For both storms, the contribution from the Soča River was highest, however it is evident that the response at the well to the second storm was not equivalent to that of the first event. During the first storm event in 2000 the Soča River end member contributed 41% of the event water, with the anthropogenic end member contributing approximately 34% and the karst water end member contributing 25%. For the second storm event, the proportion contributed by the Soča River end member was similar to that of the first event (43%), while the contributions from the karst water component decreased and that of the anthropogenic component increased until the proportions of the two were nearly

 DOI 10.1007/s10040-006-0031-6

Table 7 Least-squares regression coefficients between EMMA model and observed data

Year	Ca	Mg	Cl	$\delta^{18}O$	EC	$\delta^{13}C_{DIC}$
r^2 (2000)	0.57 (0.85)[a]	0.97 (0.98)	0.98 (0.92)	0.94 (0.92)	0.93	0.62
r^2 (1999)	0.89	0.99	0.86	0.84	–	–

[a] Values in parentheses represent the data analysis performed on the 2000 storm data with the 4 parameters Ca, Mg, Cl and $\delta^{18}O$ only

equal (29 and 28%, respectively). In the second storm event, the contribution from the anthropogenic component was greater at the beginning of the event, likely due to the elevated hydraulic head conditions resulting from the previous storm.

Figure 8b shows the results of the end-member proportions for the storm event of 1999. These proportions were summed in the same manner as the results from the 2000 events. For the 1999 event, 58% of the chemical signal was attributable to the Soča River, 10% was derived from the autogenic recharge, or karst water component, and 32% was from the anthropogenic component. In comparison to the results from 2000, the contribution from the Soča River was greater in 1999 than in 2000, while the karst water component was markedly lower and the anthropogenic component was markedly higher.

Predictive capability of the EMMA model

In order to determine how well the calculated proportions of the end-member mixtures predicted the water chemistry of the observed samples, the end members were removed from U-space and transformed back into values of concentrations of the original solutes, then "mixed" according to the proportions calculated for each observed sample. The resulting predicted chemical and isotopic values were subsequently plotted against the original data, and linear least squares regression was performed. The correlation coefficients (r^2) for each parameter are shown in Table 7. The calculated and observed values were also plotted together in time series; in this way it is possible to look for temporal differences that may indicate better or poorer prediction within certain time windows during the sampling period. The results from the 2000 storm sampling at well B-4 are shown in Fig. 9, while those of the four solutes used in the analysis of the1999 storm sampling are shown in Fig. 10.

Discussion

The chemical and stable isotope chemographs of the well water reveal clear and repetitive changes in the sources of the water at the Klariči pumping station in response to precipitation events. The high r^2 values between the observed data and the predictions from the PCA/EMMA model indicate a good fit, thus the three end members chosen for the mixing model appear adequate to account for the observed well water chemistry.

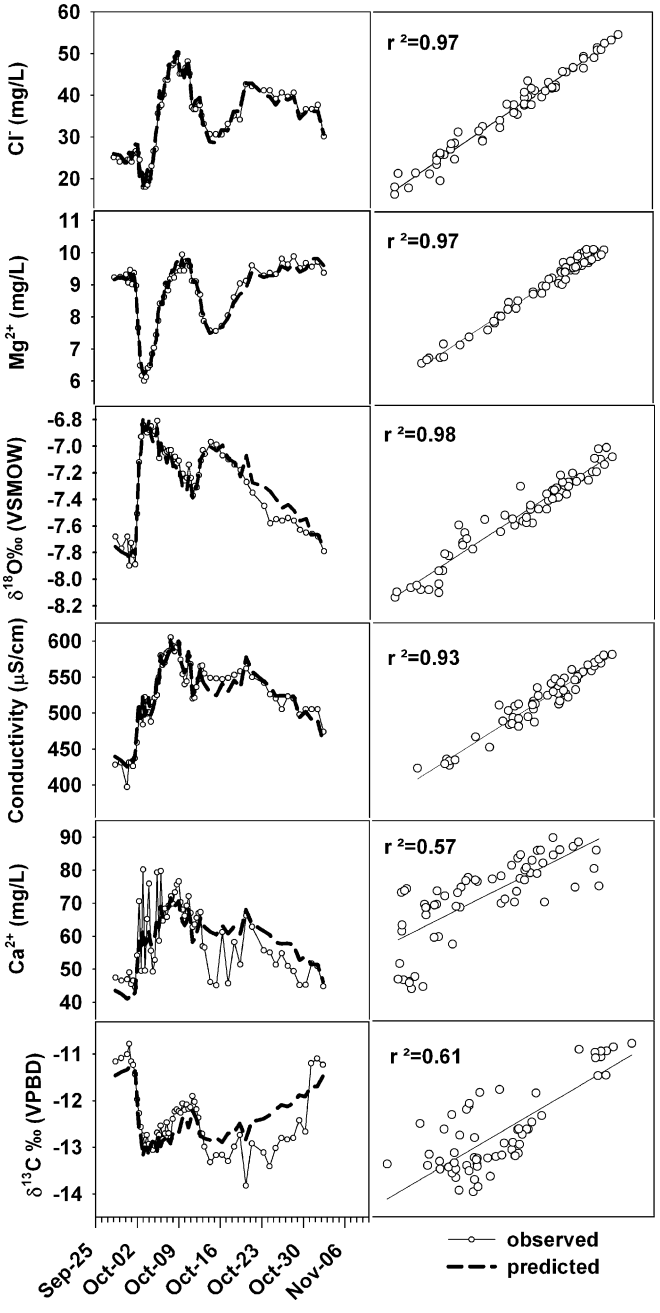

Fig. 9 Comparison of the observed and estimated chemical and isotopic parameters for the 2000 storm events at well B-4. *Left panels* are results in time series; *right panels* are linear least squares regressions, with observed values on the x-axis

 DOI 10.1007/s10040-006-0031-6

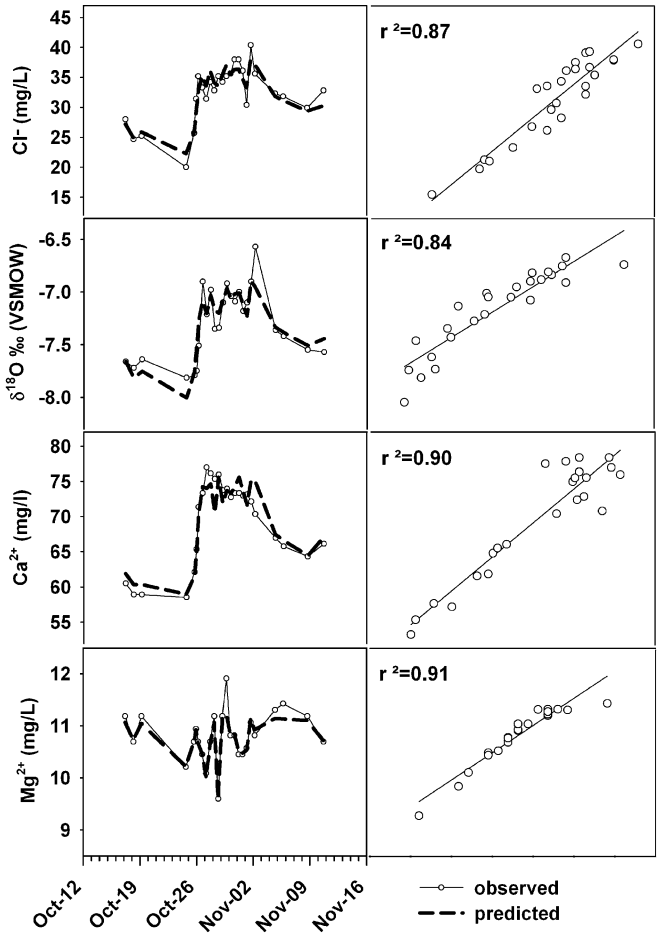

Fig. 10 Comparison of the observed and estimated chemical and isotopic parameters for the 1999 storm events at well B-4. *Left panels* are results in time series; *right panels* are linear least squares regressions, with observed values on the x-axis

Choice of end members in the PCA/EMMA model

The Soča River end-member water is derived from the alluvial aquifer fed by water sinking from the Soča River, and is widely believed to influence the Kras aquifer resurgence as discussed above. The general chemistry of the Soča River reflects Ca–Mg–HCO_3 water of relatively low conductivity, with an average Ca/Mg ratio (3.0) that is lower than the other groundwaters of the Kras aquifer (typically 4–6). This is due to the river recharge flowing through dolomitic rocks, from which it acquires Mg in excess of the calcium carbonate groundwaters of the local resurgence zone. The chloride concentration in the Soča River is low, averaging around 1–3 mg/L. The isotopic composition of the river water shows a strong seasonal inversion, resulting from the high elevation recharge area within the Julian Alps (elev. >2,000 m a.s.l., northwest of the Kras region) that contributes snowmelt to much of the river's discharge during the spring and summer months (Flora and Longinelli 1989). Thus, the oxygen isotopic composition of the river is distinctly more depleted in ^{18}O than groundwaters derived from local autogenic recharge.

The chemical and isotopic compositions of well B-3 water were determined to be constant across different seasons and hydrological conditions (Doctor 2002). The average Ca/Mg ratio is very high (26±3, n=6), likely due to the lack of Mg-bearing minerals in the recharge zone of this well. The average $\delta^{18}O$ value of the well water (–6.5‰) reflects that of local weighted mean annual effective precipitation. Given the low hydraulic conductivity and transmissivity of the aquifer around this well, the water in the well is assumed to be representative of a diffuse-flow component of storage in the aquifer, i.e., storage within fractures and/or the rock matrix. The observed ephemeral dry conditions in the well indicates that well B-3 is finished within the zone of water table fluctuation, and therefore primarily receives karst water from the vadose zone portion of the aquifer.

Despite these two water sources seeming to account for the major chemical and isotopic compositions of groundwaters in the Kras resurgence zone, a problem remained: some of the springs and wells occasionally show concentrations of chloride elevated above those measured in the Soča River and in well B-3. Thus, a third end member was hypothesized. The third end member was not directly sampled during this study; however, its composition has been inferred from the chemistry of a nearby cave, the Timavo Fishpond Cave, located near the Timavo springs (Fig. 1). The water chemistry of this shaft was measured previously (Gemiti 1994), and in relation to the other karst groundwaters of the region this cave shows elevated concentrations of Cl^- (103 mg/L), SO_4^{2-} (35 mg/L), and the highest electrical conductivity (815 µS/cm) of all of the local groundwaters. The bi-variate plots indicate that the third end member should have $\delta^{13}C_{DIC}$ in the range of –13.0 to –14.0‰, and $\delta^{18}O$ value between –6.5 to –7.5‰. This is consistent with water residing in storage within the shallow epikarst zone, and thus supports the hypothesis that chemistry similar to that observed at the Timavo Fishpond Cave is likely to be representative of this end-member source.

Conductivity response to storms at well B-4

Conductivity responses of wells and springs to storm events have been extensively used as a first-order means of exploring relationships between flow regimes and chemistry within karst aquifers (Atkinson 1977; Scanlon and Thrailkill 1987; Hess and White 1988). The continuous conductivity record obtained at well B-4 in 2000 (Fig. 5) shows that the overall trend in the conductivity of the well water is *increasing* with increasing rainfall, punctuated by short-lived dilution immediately following the most intense events (>20 mm rainfall in 24 h). The highest value of conductivity recorded by the probe inside the well was 737 µS/cm. This conductivity value is more than twice as high as other values observed in the karst groundwaters nearby. The high conductivity water at well B-4 coincides with high concentrations of Cl^-, therefore the reservoir of this unknown solution is likely to be the

 DOI 10.1007/s10040-006-0031-6

same as that which yields the elevated Cl^- observed at the caves intersecting the water table nearby.

Carbonate chemistry and $\delta^{13}C_{DIC}$ evolution during storms

$\delta^{13}C_{DIC}$ is a useful tracer of waters in the vadose zone due to the separation between the $\delta^{13}C_{DIC}$ values of waters that evolve under different conditions with respect to soil CO_2. Deines et al. (1974) present a comprehensive discussion on the $\delta^{13}C_{DIC}$ evolution of carbonate groundwaters. They showed that the variability in $\delta^{13}C_{DIC}$ depends primarily upon PCO_2 and pH for given $\delta^{13}C$ values of soil CO_2 and of carbonate rock. Their model assumed no influence of carbonate rock on the $\delta^{13}C$ value of DIC during open-system carbonate solution, such that isotopic equilibrium is maintained between the reservoir of soil CO_2 and the aqueous carbonate species, while under closed-system conditions the $\delta^{13}C$ evolution of the DIC in the water is influenced both by equilibrium with soil CO_2 and the addition of carbon from carbonate mineral dissolution. They reported that for carbonate groundwaters in the Nittany Valley karst of Pennsylvania, USA, most of the diffuse-type wells and springs exhibit $\delta^{13}C_{DIC}$ compositions in the range of –12 to –14‰, with an average of –13.3‰. Based on their modeling efforts, they concluded that the groundwaters that fell within this range achieved $\delta^{13}C_{DIC}$ via closed-system dissolution of carbonate rock, while waters that evolved under open-system conditions exhibit lighter $\delta^{13}C_{DIC}$ values, in the range between –15 to –20‰ with an average of –18‰.

Measurements of the $\delta^{13}C$ of soil CO_2 at the well B-4 and well B-3 sites in September 2000 at a depth of 0.5 m were –20 and –22‰, and $\delta^{13}C$ of carbonate rocks from the sites were –1.6 and –2.0‰, respectively. The mean $\delta^{13}C_{DIC}$ value of well B–3 is –13.8±0.5‰ (n=12), which is in agreement with the model results of Deines et al. (1974) for closed-system carbon isotopic evolution of the groundwater. However, the well B-3 is in a zone of fluctuating water table and occasionally is dry, thus it cannot be considered as a totally closed system with respect to a gas phase. More likely, water in this well represents a "medium system condition" resulting from a mixture between open system carbonate dissolution combined with closed system carbonate dissolution (Staniaszek and Halas 1986). Regardless of its evolution, the $\delta^{13}C_{DIC}$ composition of well B-3 remained nearly constant throughout 2 years of sampling, and is the most depleted of all of the waters analyzed in the Kras aquifer resurgence zone (Doctor 2002).

Figure 11 shows the evolution of the carbonate chemistry at well B-4 during the storms of 2000. During the rising limb of storms, the $\delta^{13}C_{DIC}$ values of the well water decreased, while PCO_2 increased in both of the first two events of 2000. This highlights the rapid contribution of water held in storage in the vadose zone to the conduit system intersected by the well. Before the onset of rainfall, the well water exhibited moderate PCO_2, moderate subsaturation with respect to calcite, the lowest Ca^{2+} concentrations, and the highest $\delta^{13}C_{DIC}$ values. After rainfall, the water composition shifted toward higher PCO_2, lower calcite saturation, higher Ca^{2+} concentrations, and lower $\delta^{13}C_{DIC}$ values. The chemistry gradually shifted back toward the initial composition during recession. This pattern repeated during the second storm event. At the end of the recession of the second storm event, the carbonate chemistry of the well was similar to that observed before the onset of rainfall. These patterns do not indicate rapid infiltration of rainfall; rather, they suggest flushing of water out of the epikarst.

Karst hydrologic processes revealed

The changing proportions of end-member components shown in time series in Fig. 8 are particularly illustrative of shifting sources of water that contribute to the well during storm events. During low water stage, the first storm event after a prolonged dry period in 2000 (Fig. 8a) caused water to be released from the "clean" reservoir of storage within the epikarst. During recession, this component was replaced by a second component of water held in epikarst storage, one that has been evidently impacted by anthropogenic pollutants. The changes in end-member proportions from the 1999 events (Fig. 8b) are muted relative to those in 2000; more importantly, the contribution from the anthropogenic component is distinctly elevated across the 1999 sampling period relative to what was observed in 2000. This is due to (1) the difference in antecedent hydrologic conditions prior to the sampling campaigns in both years (sampling in 1999 began in the midst of the wet period, whereas in 2000 sampling began after a prolonged dry period), and (2) the rain events in 2000 were much larger than those in 1999. For 2000, it is evident that the second and third events were more similar to the 1999 response after the system had been "primed" to a wetter condition following the first event.

The changing contribution of the anthropogenic end member is indicative of the shallow epikarst circulation hypothesized by Gemiti (1994). Water from this localized reservoir is routed to the well B-4 when the local hydraulic head is elevated—an example of karstic overflow. It is of particular importance to note how quickly changes in end-member components occur at this water supply well, especially after the dry period in 2000. The first major rainfall caused a rapid (within hours) influx of water derived from autogenic recharge into the conduit network that feeds the well, followed by a second contribution of shallow groundwater that increased during the recession limb of the first storm. This rapid increase in the karst water component can be interpreted as the first pressure pulse forcing water out of diffusive storage and into the conduit system. As this initial pressure wave passes, the karst water is progressively replaced by water from the shallow circulation system containing the high Cl^- end member as the local hydraulic head increases.

The influence of epikarst water observed during storm events at this site initially seems to contrast with results reported by Vesper and White (2004) for a spring system

 DOI 10.1007/s10040-006-0031-6

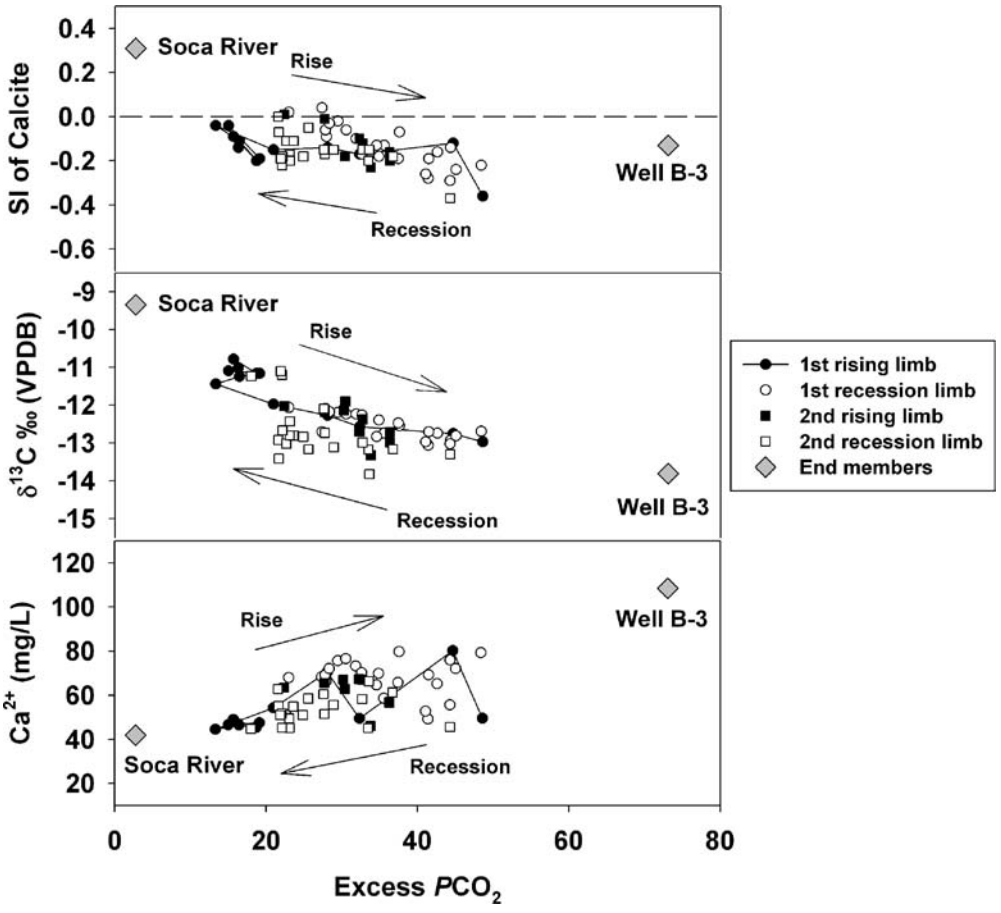

Fig. 11 Carbonate chemistry evolution of well B-4 during storm events of 2000. The correspondence of increasing PCO_2, lower SI of calcite, lower $\delta^{13}C_{DIC}$, and greater Ca^{2+} concentrations during the rising limb of the storm events indicates increased contributions from epikarstic water

in northern Tennessee, USA. They attribute the dilution observed in their spring chemographs on the rising limb to quickflow recharge by routing of surface water through sinkholes into the conduit system. Whereas the results of Vesper and White (2004) show specific conductivity and discharge to be out of phase at the spring they studied, the records at the well B-4 show specific conductivity to be in phase with discharge at the nearby Timavo springs. However, once the system is sufficiently wet, large rain events do indeed cause initial short-term dilution of water chemistry at well B-4 on the rising limb, as shown by the sharp dips in the extended EC record during the November floods of 2000 (Fig. 5). Thus, some fraction of recently recharged water arrives at the well within several hours after rainfall. This is in accordance with the conceptual model of Vesper and White (2004) that envisions fast flowpaths routing surface runoff quickly into conduits, followed by increasing contributions from dispersed sources of infiltration derived from soil and/or epikarst storage during recession. In fact, the EC being in phase with the discharge at well B-4 is the result of water released from epikarst storage, reflecting in this case the additions of the high-chloride end-member stored within the epikarst that is routed to the well with rising hydraulic head.

In general, the EMMA model best predicts the values of Mg^{2+}, Cl^-, $\delta^{18}O$, and EC, while it provides a poorer prediction of Ca^{2+} and $\delta^{13}C$ values. The high variability in Ca^{2+} concentrations during the rising limb of a storm is likely the result of flushing waters from fine fractures that achieve variable saturation states with respect to calcium carbonate, particularly during those events that occur during the driest antecedent conditions (see Fig. 4b). In the later-time recession of the 2000 storm events, the $\delta^{13}C_{DIC}$ remained lower than prior to the storm events. This may be due to a greater proportion of soil CO_2 influencing the DIC after a storm, thus causing the $\delta^{13}C_{DIC}$ value of this end-member to be lower than estimated by the end-member mixing model. Higher PCO_2 values after the storms than those prior to rainfall support this interpretation.

Although the Soča River loses a large fraction of its flow, it is not representative of losing streams typically found in karst terrains that lose flow at specific sink points. Rather, this river supports a large regional alluvial aquifer system. Water stored in the alluvial aquifer sinks into conduits in the underlying carbonate bedrock, thus the alluvial aquifer system also supplies phreatic allogenic water to the karst aquifer. As a result, variations in the losses of the Soča River are damped by the storage in the alluvial aquifer, and are not evident on the time scale of storm event sampling. It is noteworthy that the water of the deeper circulation system derived from the Soča River does not return to its prior dominance during the recession period, but that its influence is progressively lessened as the influence of the shallow epikarstic circulation system

 DOI 10.1007/s10040-006-0031-6

around the supply well increases with successive storms. This implies that local rainfall entering the shallow circulation system can provide sufficient hydraulic head so as to inhibit the expression of the deeper phreatic water, and has significant implications for well-head protection. The shallow flow system appears to have a high and prolonged impact on this water supply during and following events, and carries the greatest potential for contributing anthropogenic pollutants under persistent conditions of elevated hydraulic head.

Conclusions

The results of the storm event separation at this well indicate that between 21 and 32% of the well water is derived from an anthropogenic component during large recharge events, when Cl concentrations reach over 50 ppm. The source is apparently linked to the local shallow vadose-zone circulation in and around the resurgence zone. This reservoir seemingly acts as an overflow to the well B-4 when there is heavy rain, and is large enough such that it is not depleted with even extreme rainfall events. Further testing for pathogens and chemical measurements of the springs, wells, and caves in the vicinity of well B-4 may help to better characterize and delineate the extent of this high-chloride component, and to develop well-head protection strategies for the pumping well at Klariči. Artificial tracer tests linking local caves and shafts to the Klariči pumping well may shed light on the pathways of overflow to this well during recharge events.

In general, increasing contributions from vadose zone storage with storm events were observed, as documented previously (Lastennet and Mudry 1997; Emblanch et al. 2003; Vesper and White 2004). However, high-frequency (at least daily) sampling of storm events using a combination of natural tracers in a PCA/EMMA model has shed additional light on the proportions of water observed at the well from distinct reserves in the karst aquifer. It was determined that a component derived from shallow vadose-zone storage is expressed immediately following intense rainfall, and is gradually replaced by a second epikarst water component influenced by anthropogenic activities. The influence of the anthropogenic component is greatest under conditions of greater saturation of the epikarst. It cannot be over-emphasized that antecedent conditions are important for determining the response of a karst system to recharge events.

Acknowledgements We extend our thanks to Kraški Vodovod of Sežana, Slovenia and Azienda Comunale Elettricità Gas ed Acqua (ACEGA) Trieste, Italy for granting access to the sampling sites and for assisting in sample collection. Precipitation samples collected for isotopic analysis by GeoKarst Engineering srl, Trieste, Italy are gratefully acknowledged. Funding for this work was provided by the US Fulbright Program, the US David L. Boren Fellowship Program, the Department of Geology and Geophysics at the University of Minnesota, and the Jožef Stefan Institute, Slovenia.

References

Andreo B, Carrasco F (1999) Application of geochemistry and radioactivity in the hydrogeological investigation of carbonate aquifers (Sierra Blanca and Mijas, Spain). Appl Geochem 14:283–299

Atkinson TC (1977) Diffuse flow and conduit flow in limestone terrain in the Mendip Hills, Somerset (Great Britain). J Hydrol 35:93–110

Azienda Comunale Elettricità Gas ed Acqua (ACEGA) Trieste (1988) Il problema dell'acqua nella provincia di Trieste (The problem of water in the province of Trieste). Arti Grafiche Smolars, Trieste, p 28

Burns DA, McDonnell JJ, Hooper RP, Peters NE, Freer JE, Kendall C, Beven K (2001) Quantifying contributions to storm runoff through end-member mixing analysis and hydrologic measurements at the Panola Mountain Research Watershed (Georgia, USA). Hydrol Proc 15:1903–1924

Cancian G (1987) L'idrologia del Carso goriziano-triestino tra l'Isonzo e le risorgive del Timavo (The hydrology of the Gorizia-Trieste karst between the Isonzo and the Timavo springs). Studi Trentini Sci Natur 64:77–98

Cancian G (1988) Significato idrologico della concentrazione di ossigeno e anidride carbonica nelle acque sotteranee tra il lago Doberdò e le risorgive del Timavo (Hydrologic significance of the concentrations of oxygen and carbon dioxide in the ground water between Lake Doberdò and the Timavo springs). Mondo Sottorraneo 12(1–2):11–29

Christophersen N, Hooper RP (1992) Multivariate analysis of stream water chemical data: the use of principal components analysis for the end-member mixing problem. Water Resour Res 28:99–107

Civita M, Cucchi F, Eusebio A, Garavoglia S, Maranzana F, Vigna B (1995) The Timavo hydrogeologic system: an important reservoir of supplementary water resources to be reclaimed and protected. Proc Int Symp "Man on Karst", Postojna, 1993. Acta Carsolog 24:169–186

Cucchi F, Pirini Radrizzani C, Pugliese N (1987) The carbonate stratigraphic sequence of the Karst of Trieste (Italy). Proc Int Symp Evolution of Karstic Carbonate Platform: Relation with other Peridadriatic Carbonate Platforms. Mem Soc Geol It 40:35–44

Deines P, Langmuir D, Harmon R (1974) Stable carbon isotope ratios and the existence of a gas phase in the evolution of carbonate ground waters. Geochim Cosmochim Acta 38:1147–1164

Desmarais K, Rojstaczer S (2002) Inferring source waters from measurements of carbonate spring response to storms. J Hydrol 260:118–134

Doctor DH (2002) The Hydrogeology of the Classical Karst (Kras) Aquifer of southwestern Slovenia. PhD Thesis, University of Minnesota, Minneapolis, MN

Doctor DH, Alexander EC Jr (2005) Interpretation of water chemistry and stable isotope data from a karst aquifer according to flow regimes identified through hydrograph recession analysis. In: Kuniansky EL (ed) US geological survey scientific investigations report 2005–5160. USGS, Reston, VA, pp 82–92

Doctor DH, Lojen S, Horvat M (2000) A stable isotope investigation of the Classical Karst aquifer: evaluating karst ground water components for water quality preservation. Acta Carsolog 29(1):52–79

Emblanch C, Zuppi GM, Mudry J, Blavoux B, Batiot C (2003) Carbon 13 of TDIC to quantify the role of the unsaturated zone: the example of the Vaucluse karst system (southeastern France). J Hydrol 279:262–274

Epstein S, Mayeda TK (1953) Variations of ^{18}O of waters from natural sources. Geochim Cosmochim Acta 4:213–224

Ford DC, Williams PW (1989) Karst geomorphology and hydrology. Hyman, London

Flora O, Longinelli A (1989) Stable isotope hydrology of a classical karst area, Trieste, Italy. In: Isotope Techniques in the Study of

Fractured and Fissured Rocks, International Atomic Energy Agency (IAEA), Vienna
Galli M (1999) Timavo: Esplorazione e studi (Timavo: exploration and studies). Supplemento no. 23 di Atti e Memorie della Commissione Grotte "Eugenio Boegan", Trieste, p 195
Gehre M, Hoefling R, Kowski P (1996) Methodical studies for D/H-isotope analysis: a new technique for the direct coupling of sample preparation to an IRMS. Isot Environ Health Stud 32:335–340
Gemiti F, Licciardello M (1977) Indagini sui rapporti di alimentazione delle acque del Carso triestino e goriziano mediante l'utilizzo di alcuni traccianti naturali (Investigations of the relations of waters feeding ground water of the Gorizia and Trieste karst using some natural tracers). Annali Gruppo Grotte Ass 30° Ott Trieste 6:43–61
Gemiti F (1984a) La portata del Timavo alle risorgive di S. Giovanni di Duino (The discharge of the Timavo at the springs of San Giovanni di Duino). Annali Gruppo Grotte Ass 30°Ott Trieste 7:23–41
Gemiti F (1984b) Nuova ed originale prova di marcatura delle acque del Timavo (A new and original trace of the water of the Timavo). Annali Gruppo Grotte Ass 30°Ott Trieste 7:43–62
Gemiti F (1994) Indagini idrochemiche alle risorgive del Timavo (Hydrochemical investigations of the Timavo springs). Atti e Memorie della Commissione Grotte "E. Boegan" 30:73–83
Hess JW, White WB (1988) Storm response of the karstic carbonate aquifer of southcentral Kentucky. J Hydrol 99:232–235
Kranjc A (ed) (1997) Slovene Classical Karst: "Kras". Institut za raziskovanja krasa ZRC SAZU, Postojna, p 254
Krivic P (1981) Etude hydrodynamique d'un aquifère karstique côtiere: le Kras de Slovenie, Yougoslavie (Hydrodynamic study of a coastal karst aquifer: the Kras of Slovenia, Yugoslavia). PhD Thesis, Accadèmie Montpellier, Univ. Sci. Tech. Languedoc, France
Krivic P (1982) Variations naturelles de niveau piézométrique d'un aquifère kartsique (Natural variations of piezometric level of a karstic aquifer). Geologija 25(1):129–150
Krokos A (1998) Ulteriori studi geochimico-isotopici su alcune sorgenti carsiche costiere dell'area triestina: considerazioni idrologico-ambientali (Further geochemical-isotopic studies of some coastal karstic springs in the area of Trieste: hydrologic-environmental considerations). Bachelor's Thesis, University of Trieste, Italy
Laaksoharju M, Skårman C, Skårman E (1999) Multivariate mixing and mass balance (M3) calculations, a new tool for decoding hydrogeochemical information. Appl Geochem 14:861–871
Lakey B, Krothe NC (1996) Stable isotopic variation of storm discharge from a perennial karst spring, Indiana. Water Resour Res 32:721–731
Lastennet R, Mudry J (1997) Role of karstification and rainfall in the behavior of a heterogeneous karst system. Environ Geol 32 (2): 114–123
Lee ES, Krothe NC (2001) A four-component mixing model for water in a karst terrain in south-central Indiana, USA: using solute concentration and stable isotopes as tracers. Chem Geol 179:129–143
Longinelli A (1988) Stable isotope hydrology of the classical Karst area, Trieste, Italy. Rendi Soc Ital Mineral Petrol 43: 1175–1183
Maloszewski P, Stichler W, Zuber A, Rank D (2002) Identifying the flow system in a karstic-fissured-porous aquifer, Schneealpe, Austria, by modeling of environmental ^{18}O and ^{3}H isotopes. J Hydrol 256:48–59
Melloul A, Collin M (1992) The 'principal components' statistical method as a complementary approach to geochemical methods in water quality factor identification; application to the Coastal Plain aquifer of Israel. J Hydrol 140:49–73
Mook WG, Brommerson JC, Staverman WH (1974) Carbon isotope fractionation between dissolved bicarbonate and gaseous carbon dioxide. Earth Planet Sci Lett 22:169–176
Mosetti F, D'Ambrosi C (1963) Alcune ricerche preliminari in merito a supposti legami di alimentazione fra il Timavo e l'Isonzo (Some preliminary research regarding a supposed connection between the Timavo and the Isonzo). Boll Geograf Teor Appl 5(17):69–84
Parkhurst DL, Appelo CAJ (1999) User's guide to PHREEQC (Version 2): a computer program for speciation, batch-reaction, one-dimensional transport, and inverse geochemical calculations. US Geological Survey Water-Resources Investigations Report. USGS, Reston, VA, pp 99–4259
Perrin J, Jeannin P-Y, Zwahlen F (2003) Epikarst storage in a karst aquifer: a conceptual model based on isotope data, Milandre test site: Switzerland. J Hydrol 279:106–124
Petrič M, Kogovšek J (2000) Guide-booklet for the excursion of the 7th COST Action 621 Management Committee and Working Groups meeting, Postojna, Slovenia. Karst Research Institute ZRC-SAZU, Postojna
Reyment R, Jöreskog KG (1993) Applied factor analysis in the natural sciences. Cambridge University Press, New York, p 371
Scanlon BR, Thrailkill J (1987) Chemical similarities among physically distinct spring types in a karst terrain. J Hydrol 89:259–279
SPSS Inc (2001) SPSS for Windows, Release 11.0.1, standard version. SPSS Inc., Chicago, IL
Staniaszek P, Halas S (1986) Mixing effects of carbonate dissolving waters on chemical and $^{13}C/^{12}C$ compositions. Nordic Hydrol 17:93–114
Stetzenbach KJ, Hodge VF, Guo C, Farnham KH, Johannesson KH (2001) Geochemical and statistical evidence of deep carbonate ground water within overlying volcanic rock aquifers/aquitards of southern Nevada, USA. J Hydrol 243:254–271
Timeus G (1928) Nei misteri del mondo sotterraneo: risultati delle ricerche idrogeologiche sul Timavo 1895–1914, 1918–1927 (Some mysteries of the underground world: results of the hydrogeologic research of the Timavo 1895–1914, 1918–1927). Atti e Mem Comm Grotte "E. Boegan" 22:117–133
Urbanc J, Kristan S (1998) Isotope investigation of the Brestovica water source during an intensive pumping test. RMZ Mater Geoenviron 45(1–2):187–191
Vesper DJ, White WB (2004) Storm pulse chemographs of saturation index and carbon dioxide pressure: implications for shifting recharge sources during storm events in the karst aquifer at Fort Campbell, Kentucky/Tennessee, USA. Hydrogeol J 12:135–143
White WB (1988) Geomorphology and hydrology of Karst terrains. Oxford University Press, New York, p 464

 DOI 10.1007/s10040-006-0031-6